Magnetite in ALH 84001: An origin by shock-induced thermal decomposition of iron carbonate

Adrian J. BREARLEY

Department of Earth and Planetary Sciences, MSC03–2040 University of New Mexico, Albuquerque, New Mexico 87131, USA
E-mail: brearley@unm.edu

Abstract–In martian orthopyroxenite ALH 84001, pockets of feldspathic glass frequently contain carbonate masses that have been disrupted and dispersed within feldspathic shock melt as a result of impact(s). Transmission electron microscope studies of carbonate fragments embedded within feldspathic glass show that the fragments contain myriad, nanometer-sized magnetite particles with cuboid, irregular, and teardrop morphologies, frequently associated with voids. The fragments of carbonate must have been incorporated into the melt at temperatures of ~900ºC, well above the upper thermal stability of siderite ($FeCO_3$), which decomposes to produce magnetite and CO_2 below ~450ºC. These observations suggest that most, if not all, of the fine-grained magnetite associated with Fe-bearing carbonate in ALH 84001 could have been formed as result of the thermal decomposition of the siderite ($FeCO_3$) component of the carbonate and is not due to biological activity.

INTRODUCTION

McKay et al. (1996) reported several lines of evidence suggesting that martian meteorite ALH 84001 may contain a fossilized record of preterrestrial life. Among the lines of evidence to support this hypothesis are the presence of fine-grained magnetite that occurs within globular-shaped, compositionally zoned carbonates that constitute ~1 vol% of the meteorite (Mittlefehldt 1994; Treiman 1995). The morphologies and grain sizes (~10–100 nm) of the magnetites were argued by McKay et al. (1996) to be typical of magnetites produced by magnetotactic bacteria on Earth. This hypothesis has, however, been challenged by Bradley et al. (1996), who found whiskers and platelets of magnetite with axial screw dislocations associated with the carbonate. Many of these grains have an epitaxial relationship with the carbonate host and have been interpreted as vapor phase condensates formed from a cooling high temperature vapor based on the presence of axial screw dislocations, which are regarded as being characteristics of crystals formed by vapor phase growth (e.g., Shaffer 1967; Veblen and Post 1983). Brearley (1998a), based on preliminary observations, suggested expanding the inorganic origin hypothesis for the origin of the magnetites in ALH 84001 that involves the thermal decomposition of Fe-bearing carbonates as a result of post-shock heating. Such a mechanism had also been alluded to by Scott et al. (1997), but no new observations to support this conjecture were presented. Golden et al. (2001) tested the

hypothesis proposed by Brearley (1998a) by carrying out an experimental study of the decomposition of Fe-bearing carbonates in synthetically grown, zoned carbonates (Golden et al. 2000). The results of these experiments are broadly consistent with the hypothesis proposed by Brearley (1998a). Similar results have also been described by Koziol and Brearley (2002) and Golden et al. (2002), and Scott and Barber (2002) have reached similar conclusions to those of Brearley (1998a) based on TEM studies of a variety of carbonate occurrences in ALH 84001. In this paper, the detailed observations of magnetite associated with carbonates in ALH 84001 that lead to the thermal decomposition hypothesis are presented, building on and expanding the preliminary results of Brearley (1998a).

Apparently, ALH 84001 has experienced a complex evolutionary history in which multiple shock events have played an important role (Treiman 1995, 1998; Scott et al. 1997, 1998; Shearer and Adcock 1998; Shearer and Brearley 1998; Greenwood and McSween 2001). These shock events appear to have occurred both pre- and post-deposition of the carbonate globules, but their possible effects on the proposed biomarkers of McKay et al. (1996) have been largely ignored. Among the effects of shock that have been recognized are the disruption and fragmentation of the zoned carbonate globules (Treiman 1995), such that the globule fragments become dispersed within the feldspathic glass (Shearer and Adcock 1998; Shearer and Brearley 1999; Greenwood and McSween 2001). The presence of veins of feldspathic glass intruding

into carbonate globules demonstrates that the dispersion of the carbonate must have occurred during shock melting of the feldspathic glass (Shearer and Adock 1998; Shearer and Brearley 1998). In contrast to previous studies of carbonates in ALH 84001 (e.g., McKay et al. 1996; Bradley et al. 1996, 1998) that have focused on intact carbonate globules, this study used scanning electron microscope (SEM) and transmission electron microscope (TEM) techniques to study the microstructures of small (<30 µm) carbonate fragments embedded within feldspathic glass. The microstructures of these carbonate grains are extremely instructive in elucidating the origin of the magnetite in ALH 84001.

ANALYTICAL TECHNIQUES

Doubly polished thin sections of sample ALH 84001,354 (mounted using an acetone soluble epoxy, Loctite 414) were prepared from a rock chip that was kindly provided by the Antarctic Meteorite Working Group. Regions of interest were selected by optical microscopy and characterized in detail by

BSE imaging using a JEOL 5800LV SEM. Slotted copper grids were glued over the areas of interest and the samples were removed by immersion in acetone. These samples were prepared for TEM by ion beam milling using a Gatan Duo ion beam mill. TEM was carried out on a JEOL 2010 HRTEM operating at 200 kV. A Link ISIS energy dispersive X-ray analysis system equipped with a Link Pentafet UTW EDS detector was used to obtain in situ mineral analyses employing the Cliff-Lorimer thin film approximation for data reduction. Experimental k-factors were used throughout.

RESULTS

SEM Observations

Previous TEM studies of ALH 84001 have focused on the large carbonate globules that occur in ALH 84001 and have been extensively described (e.g., Mittlefehldt 1994; McKay et al. 1996; Gleason et al. 1997; Scott et al. 1997, 1998). However, the focus of this study is occurrences of
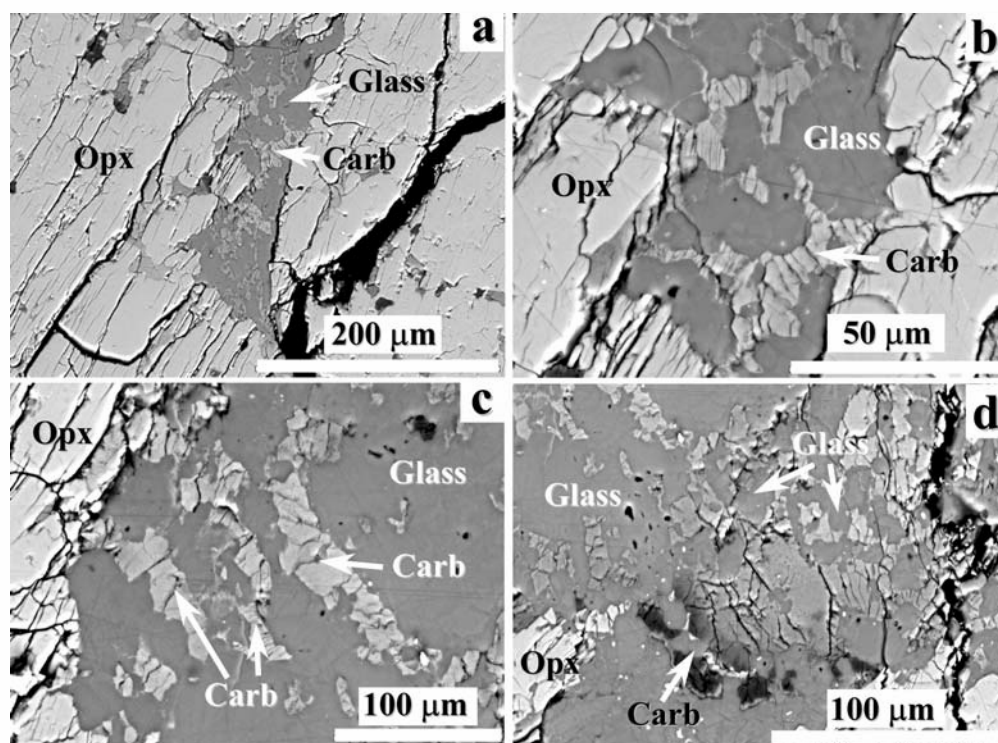

Fig. 1. Backscattered electron (BSE) images of feldspathic glass pockets that contain disrupted regions of carbonate: a) feldspathic glass pocket between 2 orthopyroxene crystals (Opx). The glass contains highly irregular regions of carbonate (Carb) that are distributed throughout the glass; b) closeup of region in (a) showing carbonate fragments that appear to have been invaded and disrupted by the feldspathic melt (now glass); c) highly disrupted region of carbonate that consists of several elongate stringers of carbonate, as well as numerous smaller fragments that are completely embedded within feldspathic glass; d) large mass of highly disrupted zoned carbonate that now consists of numerous angular fragments. The carbonate mass has been invaded and dispersed by the shock melt; e) closeup of (d) showing that the compositional zoning within the large mass of carbonate is identical to that observed within carbonate globules. The outer part of the carbonate shows 2 narrow but distinct zones of Fe-enrichment; f) small region of zoned carbonate within feldspathic glass. The right part of the image shows numerous small fragments of carbonate that have been broken off from the main carbonate mass; g) feldspathic glass pocket that consists of numerous carbonate fragments that are connected by very thin, usually continuous stringers of carbonate; h) closeup of region in (g) showing angular carbonate fragments that are connected by long, thin stringers of carbonate that extend through the feldspathic glass.

carbonate that are closely associated with feldspathic shock glass. Several regions of feldspathic glass that contained carbonate were identified using optical microscopy. As described by several authors (e.g., Treiman 1995; Scott et al. 1997, 1998; McKay et al. 1997; Greenwood and McSween 2001), such regions typically occur between large orthopyroxene crystals, some of which have been misoriented by impacts. The pockets of feldspathic glass are variable in shape and size but, in the examples studied, are typically less than 200 μm in their maximum dimension. Many of these pockets contain variable amounts of

carbonate, which is embedded within the glass (e.g., Greenwood and McSween 2001).

BSE images of typical examples of feldspathic glass that contain variable amounts of carbonate are shown in Figs. 1a–1h. The TEM observations discussed below are from these regions. From the BSE studies, the feldspathic glass clearly contains numerous regions of carbonate that typically have an angular or fragmental appearance, suggesting that they represent portions of larger masses of pre-existing carbonate. The fragments show a wide range of grain sizes, from just a few microns up to several tens of microns (e.g., Figs. 1a–1c).
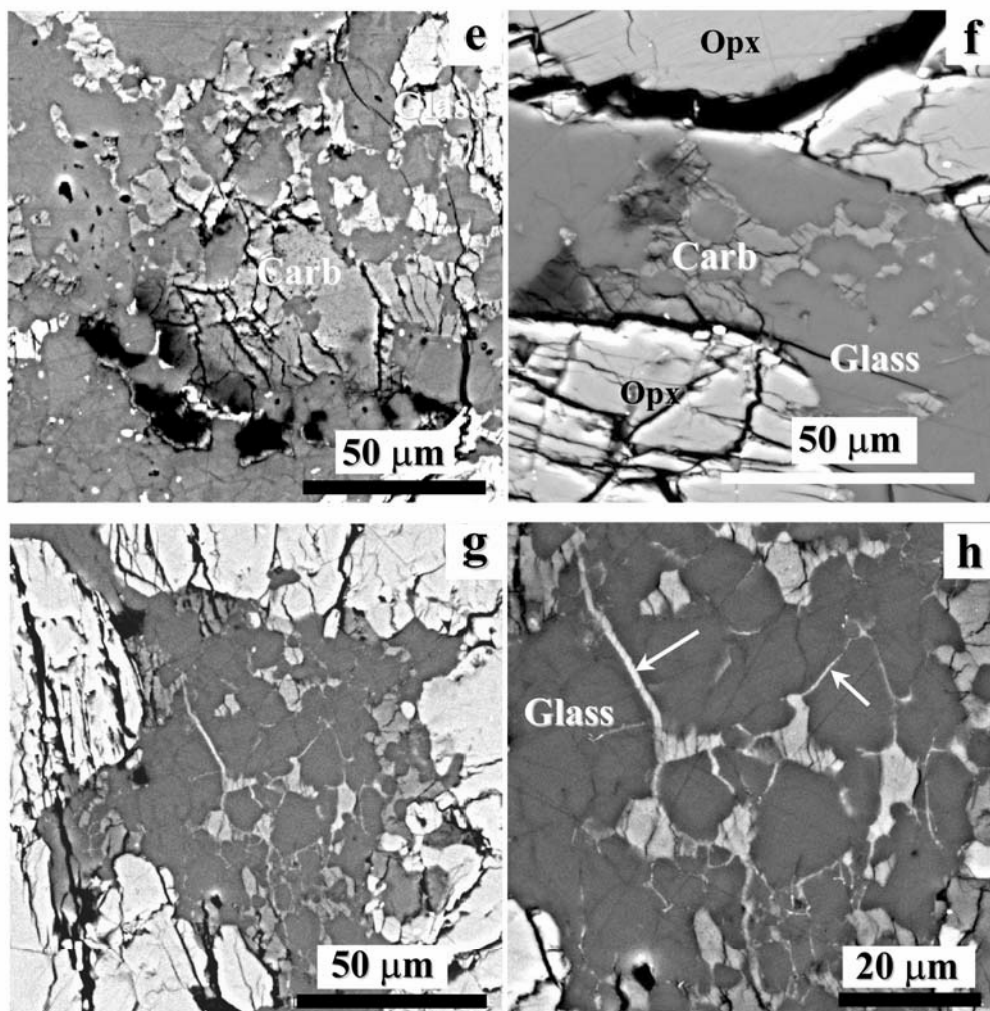

Fig. 1. Backscattered electron (BSE) images of feldspathic glass pockets that contain disrupted regions of carbonate: a) feldspathic glass pocket between 2 orthopyroxene crystals (Opx). The glass contains highly irregular regions of carbonate (Carb) that are distributed throughout the glass; b) closeup of region in (a) showing carbonate fragments that appear to have been invaded and disrupted by the feldspathic melt (now glass); c) highly disrupted region of carbonate that consists of several elongate stringers of carbonate, as well as numerous smaller fragments that are completely embedded within feldspathic glass; d) large mass of highly disrupted zoned carbonate that now consists of numerous angular fragments. The carbonate mass has been invaded and dispersed by the shock melt; e) closeup of (d) showing that the compositional zoning within the large mass of carbonate is identical to that observed within carbonate globules. The outer part of the carbonate shows 2 narrow but distinct zones of Fe-enrichment; f) small region of zoned carbonate within feldspathic glass. The right part of the image shows numerous small fragments of carbonate that have been broken off from the main carbonate mass; g) feldspathic glass pocket that consists of numerous carbonate fragments that are connected by very thin, usually continuous stringers of carbonate; h) closeup of region in (g) showing angular carbonate fragments that are connected by long, thin stringers of carbonate that extend through the feldspathic glass.

In some cases, the fragments can clearly be seen to have formed by the disruption of larger, zoned aggregates of carbonate (e.g., Figs. 1d–1f), while in other examples, the carbonate fragments are so highly dispersed that the characteristics of the original carbonate mass cannot be determined. In some rare instances, the individual carbonate fragments are connected by extremely thin (<1 μm) fingers or veins that cross cut the feldspathic glass (Figs. 1g and 1h) and give the glass a mosaic appearance. These fingers can extend through the glass for up to 30 μm but are typically <10 μm in length. McKay and Lofgren (1997) and McKay et al. (1997) have termed this texture "lacy" carbonate. High resolution BSE imaging of the interfaces between the carbonate fragments and the glass shows that they are often planar and are probably crystallographically controlled. This observation has been confirmed by TEM as discussed below. Some regions of carbonate also display embayed outlines that are suggestive of resorbtion of carbonate into the melt phase (e.g., Figs. 1c, 1d, and 1f). However, high contrast BSE images show no clear evidence of any compositional variations in the melt adjacent to the carbonate fragments to indicate that such a process has actually occurred. Most of the carbonates show evidence of complex zoning that is essentially identical to that described in other occurrences of carbonate in ALH 84001 (e.g., McKay et al. 1996; Gleason et al. 1997). Examples of well-developed compositional zoning in the carbonate fragments are illustrated in Figs. 1d, 1e, and 1f. The zoning extends across fragments that are now separated by glass, providing further evidence that the fragments once represented parts of a larger continuous mass of carbonate. Similar examples have also been described in detail by Greenwood and McSween (2001).

TEM Observations

Transmission electron microscope observations were carried out on 5 separate pockets of feldspathic glass that contain carbonate. Essentially the same microstructural characteristics were observed in the carbonates in each of the regions. Based on analytical electron microscope (AEM) analyses, the compositions of the carbonate fragments examined lie in the compositional range from ~$Cc_{33}Mg_{79}Sd_{18}$ to ~$Cc_{23}Mg_{45}Sd_{32}$ (Fig. 2), which is typical for the interior parts of carbonate globules. One very calcic carbonate fragment was also studied. On the TEM scale, the carbonate fragments typically have sharp, planar interfaces with the feldspathic glass, and these interfaces are commonly the cleavage surfaces of carbonate rhombs (i.e., [$10\bar{1}1$]) (Figs. 3a and 3b).

Imaged at low magnification, the carbonate fragments exhibit an extremely complex mottled contrast (Figs. 3 and 4), which is due to a combination of 3 different microstructural characteristics. The first of these is the fact that the carbonate fragments are extensively strained (Figs. 3a and 4) and consist
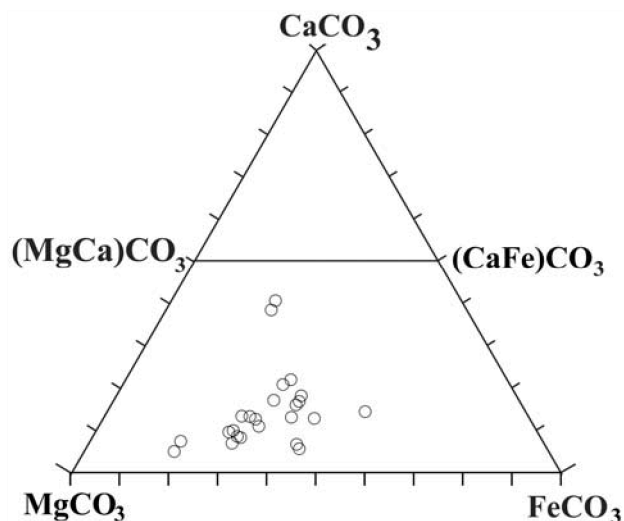

Fig. 2. $CaCO_3$-$MgCO_3$-$FeCO_3$ ternary diagram showing the range of compositions of the carbonate fragments studied by transmission electron microscopy.

of submicron domains within the grains, where the lattice is distorted and strained but apparently contains few dislocations. The domainal structure of the carbonate is illustrated by the asterism in the electron diffraction pattern in Fig. 4.

The second significant microstructural feature of the carbonate is the presence of myriad magnetite inclusions (Figs. 5a–c), most of which are randomly oriented. But, some of these inclusions have the same crystallographic orientation relationships with the carbonate as described by Bradley et al. (1996). The magnetites are relatively evenly distributed throughout the carbonate grains and show no evidence of being concentrated in particular regions (Fig. 5b), although, rare linear arrays of randomly oriented magnetite grains have been observed. The magnetites occur exclusively within the carbonate and have never been observed within the associated glass. Magnetite grain sizes range from <10 nm up to 100 nm.

Detailed descriptions of the morphological characteristics of magnetites in ALH 84001 have been presented by Thomas-Keprta et al. (2000, 2001), following the work of McKay et al. (1996). All the different morphologies described by McKay et al. (1996) and Thomas-Keprta et al. (2000) are present in the carbonate fragments studied here, including cuboid, teardrop, whisker, irregular, hexagonal, and platelet morphologies (Fig. 6). All the different morphologies typically occur within the same carbonate fragment, including examples of the parallelpiped morphology that have been specifically attributed to the activity of magnetotactic bacteria (Thomas-Keprta et al. 2000, 2001).

The bulk of the magnetite grains are defect free. But, rare and more complex grains have also been observed, as shown in Fig. 7. Figure 7a shows a composite grain that consists of 2 separate domains with distinct orientation relationships, as
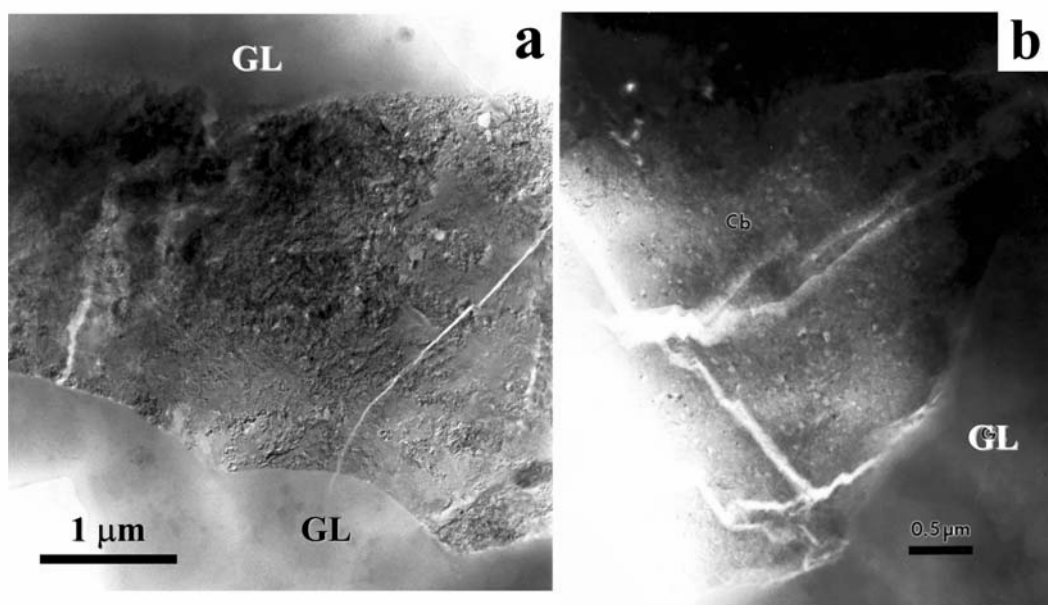
Fig. 3. Transmission electron microscope images of the microstructures of carbonate fragments: a) low magnification, bright field TEM image of part of a carbonate fragment embedded within feldspathic glass (GL). The complex microstructure of the carbonate is due to a high degree of strain within the carbonate. Inclusions of magnetite are also present but are less abundant than in other fragments (e.g., Fig. 3b). The interface between the carbonate and the glass is extremely sharp and well-defined and tends to be either planar or slightly curved. The planar interfaces are typically the cleavage planes of the carbonate grain; b) low magnification bright field image of a carbonate fragment embedded within feldspathic glass (GL). The fragment has a complex mottled appearance that is caused by the presence of myriad magnetite crystals and voids that are distributed at a very high density through the carbonate grain. The fractures are cleavage planes within the carbonate that have probably opened up during sample preparation.
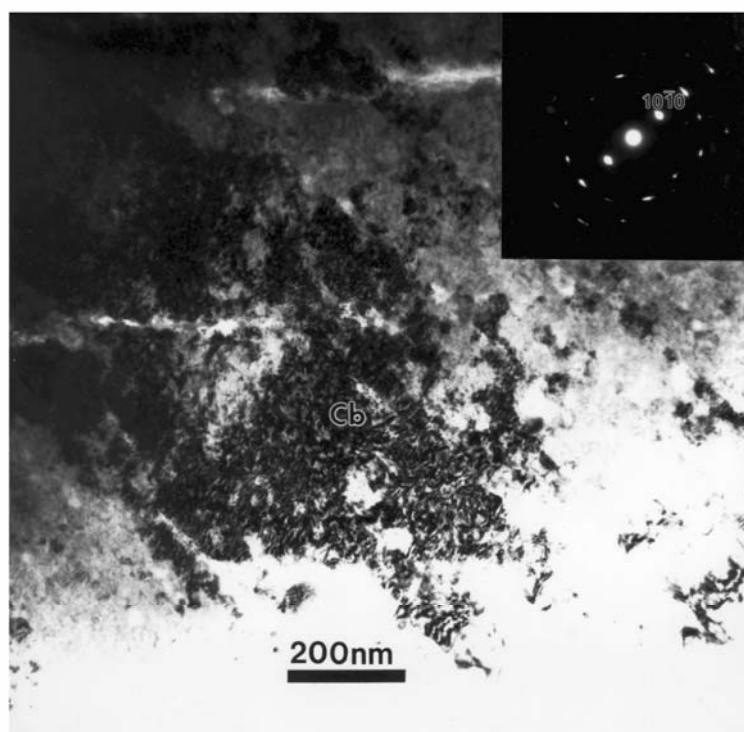

Fig. 4. Bright field TEM image of a fragment of carbonate that shows a pronounced domainal microstructure and complex strain contrast. The presence of different domains and localized strain within the carbonate lattice causes the asterism in the diffraction maxima in the inset electron diffraction pattern (upper right).
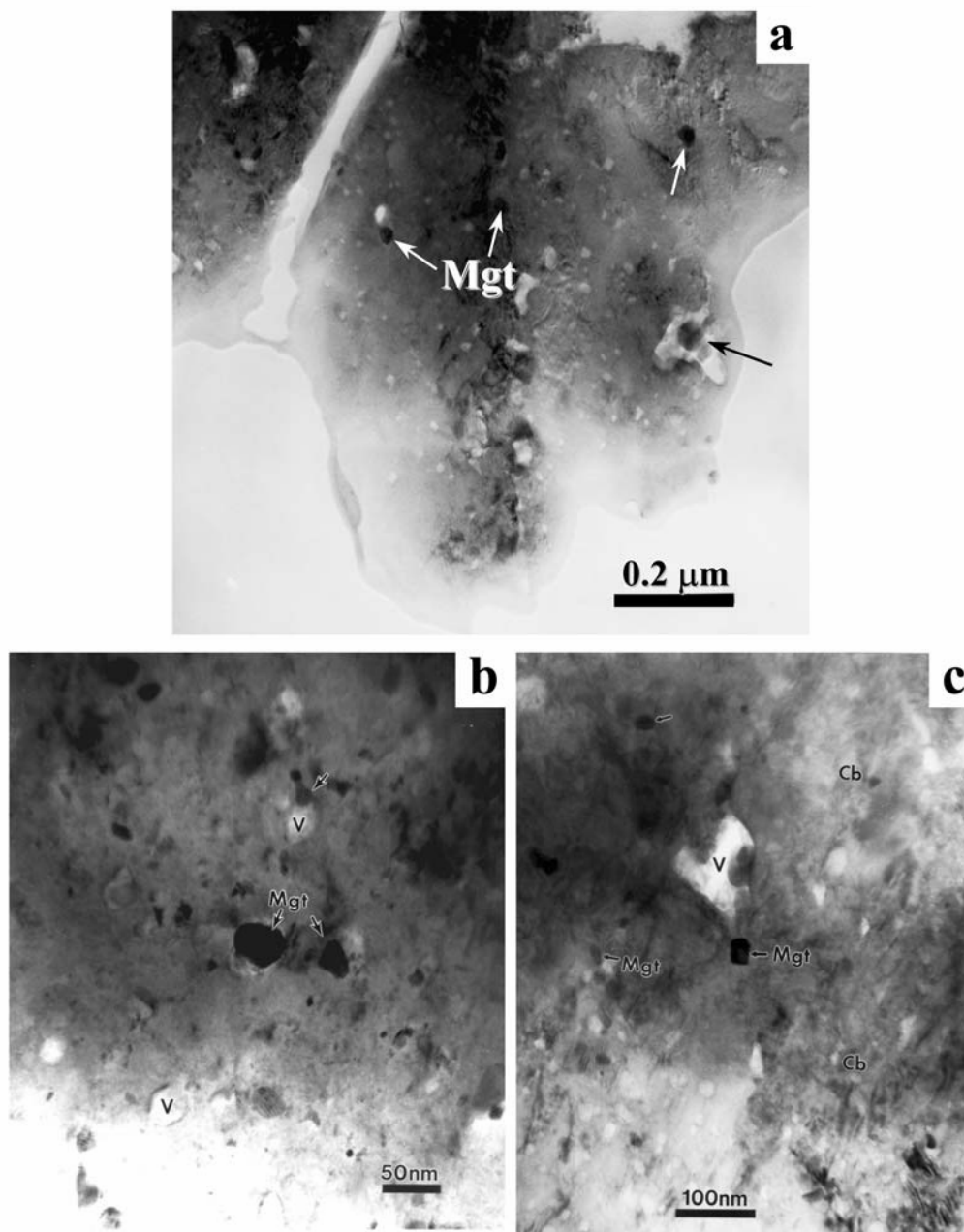
Fig. 5. a) Bright field TEM image of a carbonate fragment that contains myriad nm-sized magnetite (Mgt) crystals, some of which are diffracting strongly and appear dark in the image (arrowed). The very small, lighter-colored regions in the carbonate are voids that give the carbonate a porous appearance; b) higher magnification bright field image of a carbonate fragment showing the presence of abundant magnetite crystals, dispersed randomly within the carbonate fragments. The high abundance of magnetite is typical for many of the carbonate fragments examined. The magnetite (Mgt) shows a variable grain size, but the grains rarely exceed 50 nm in diameter. Numerous voids (V) are also distributed throughout the region of carbonate (Cb); c) highly strained region of carbonate that contains numerous inclusions of magnetite. A large, irregularly-shaped void (V) is located in the upper central part of the image.

shown by the associated electron patterns for each domain. Fig. 7b shows a more complex example in which one half of the grain is defect-free, while the second half is a domain in a different crystallographic orientation that contains numerous stacking faults that cause streaking in diffraction maxima in electron diffraction patterns.

The most common occurrence of magnetite is as individual grains embedded within the carbonate. However, we have also observed occurrences where several grains of magnetite occur together, as shown in Figs. 8a–8c, usually associated with a large void. Figures 8a and 8c show examples of clusters of magnetite where at least one of the
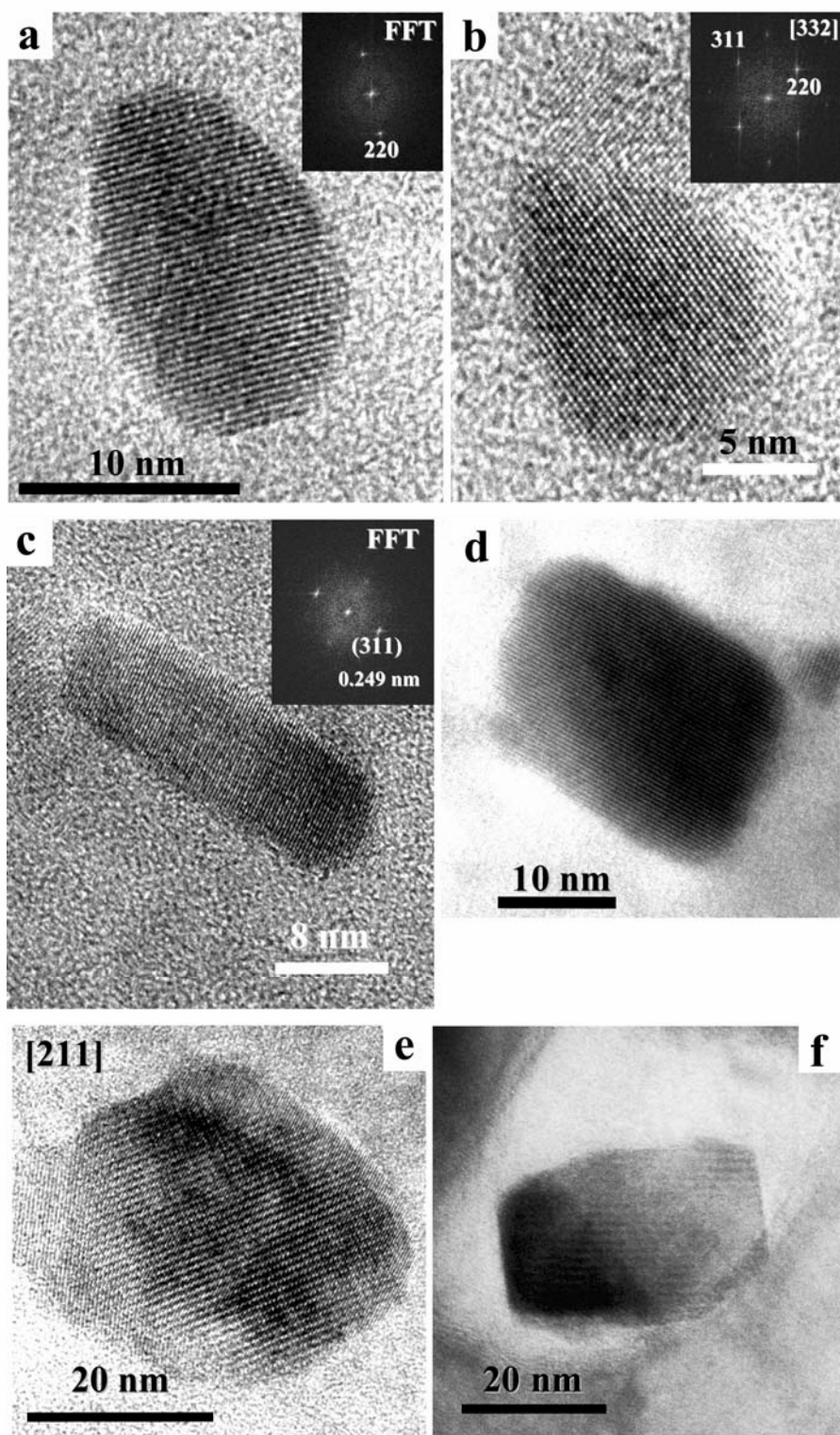
Fig. 6. High resolution TEM images showing the range of morphologies of magnetite that have been observed within the carbonate fragments: a) magnetite with teardrop morphology. The inset shows the electron diffraction patterns (FFT—fast fourier transform of the TEM image), which show (220) reflections; b) high resolution image of an irregularly-shaped magnetite crystal oriented parallel to the [332] zone axis. The inset is the FFT diffraction pattern for the crystal; c) elongate crystal of magnetite with the (311) 0.249 nm lattice planes resolved; d) magnetite crystal with prismatic morphology; e) high resolution TEM image of a hexagonal magnetite particle imaged down the [211] zone axis; f) magnetite with a parallelpiped morphology.
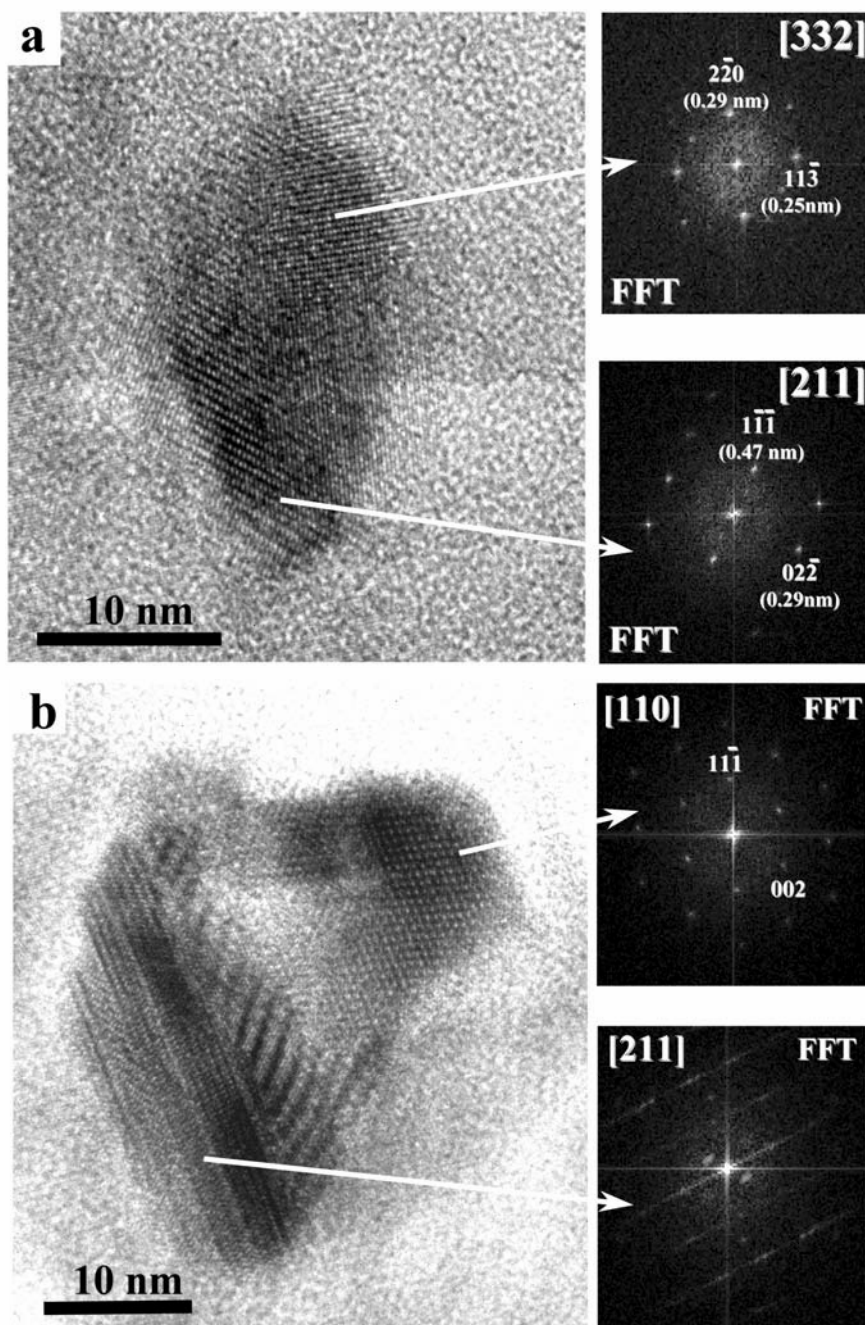
Fig. 7. High resolution TEM image of complex magnetite grains in carbonate fragments in ALH 84001: a) composite grain that consists of 2 different domains that are misoriented with respect to one another. Inset FFT diffraction patterns show the orientations of each of the distinct domains, e.g., [332] zone axis for the upper domain and [211] zone axis for the lower domain; b) composite magnetite grain consisting of a domain on the right of defect-free magnetite in the [110] orientation (FFT, upper right). The part of the grain on the left contains several stacking faults and the diffraction maxima (FFT, lower right) show considerable streaking.

crystals is a facetted whisker similar to those described by Bradley et al. (1996). The whiskers appear to have nucleated on the void walls and grown outward into the void space. In comparison, in Fig. 8b, the magnetites that surround a central void all have irregular morphologies. Note that the voids associated with clusters of magnetite are significantly larger than those associated with single carbonate grains (see below).

The final distinct feature of the carbonate is the presence of abundant nm-sized voids, which gives the carbonate a porous appearance (Fig. 9). Such voids have also been described in the larger carbonate globules (McKay et al.
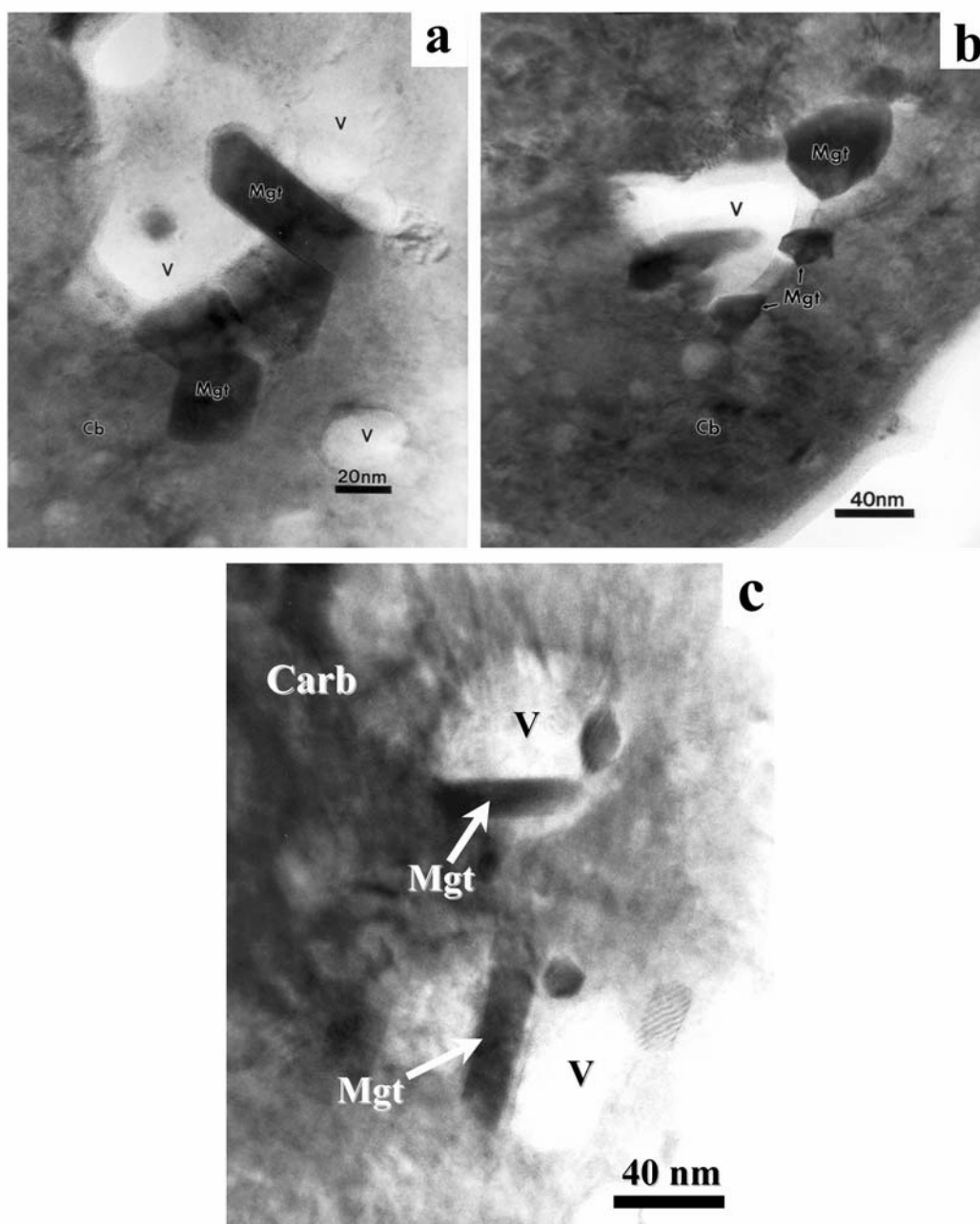
Fig. 8. Bright field transmission electron micrographs of clusters of magnetite crystals related to large voids in ALH 84001: a) region of carbonate (Cb) with a number of separate magnetite crystals (Mgt) associated with a central void (V). One of the magnetites has a whisker morphology with well-developed facets and appears to have grown out from the void wall. Several other voids are closely related to the cluster of magnetite crystals; b) group of irregularly-shaped magnetites with variable sizes clustered around a large central void. The carbonate in this region is highly strained and contains numerous smaller voids with sizes that range down to <5 nm; c) region of carbonate (Cb) that contains 2 (V) voids with associated magnetite (Mgt) crystals. In both voids, magnetite whiskers are present. Note the hexagonal outline of the smaller crystal in the lower void.

1996; Bradley et al. 1996; Blake et al. 1998). The voids range from <10 nm up to 70 nm, and most of them are associated with individual magnetite grains (Figs. 10a–10d), although, many of the smallest voids show no evidence of being associated with magnetite. Voids in the smaller size range typically have a subrounded or oval shape (Fig. 11a) but may

also be partially facetted with a shape similar to that of carbonate rhombs. High-resolution imaging and electron diffraction patterns show that the walls of the voids are rational crystallographic planes, which are invariably the cleavage planes of rhombohedral carbonate (e.g., $[10\bar{1}1]$) (Fig. 12).
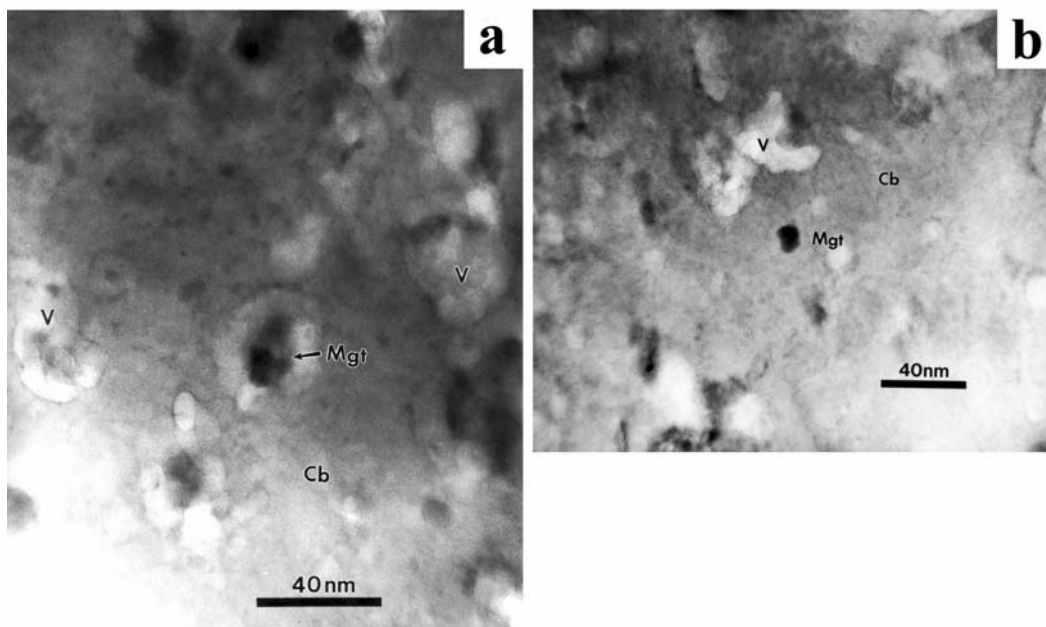
Fig. 9. Bright field transmission electron micrograph showing the porous structure of carbonate in ALH 84001: a) region of carbonate (Cb) with a high density of irregularly shaped voids (V) that appear as light colored regions within the carbonate. The magnetite (Mgt) grain in the center of the image is surrounded by several voids that appear to have partially coalesced around the grain; b) region of carbonate that contains numerous voids, such as the highly irregular void in the upper center. Dark crystals of magnetite (Mgt) are distributed throughout the magnetite but at a lower density than in other regions of carbonate.

DISCUSSION

Carbonates in ALH 84001 have been studied extensively by a variety of workers, but the bulk of the SEM, microprobe, and TEM studies have concentrated on the distinctive carbonate globules. The observations presented here are on an occurrence of carbonate that has not received such close scrutiny by TEM, although SEM and electron microprobe studies have been performed (e.g., McKay and Lofgren 1997; Greenwood and McSween 2001). TEM studies of this occurrence of carbonate provide some very useful insights into the observations that were made by McKay et al. (1996) and have been interpreted as being indicative of a biological origin. Here, I discuss the implications of these observations on the possible genesis of magnetites in ALH 84001.

McKay et al. (1996) studied magnetites that occur exclusively in 2 distinct zones of very Fe-rich carbonate within carbonate globules, one located in a thin band at the rim of the globule and a second located more towards the interior of the carbonate. Although the compositions of these Fe-rich carbonate bands were not reported, based on compositional profiles across a similar carbonate globule in ALH 84001 (Shearer et al. 1997), they probably have a composition close to $Cc_{12}Mg_{44}Sd_{44}$. The composition of these growth zones is consequently about 10 mol% richer in siderite than the next most Fe-rich carbonate composition in ALH 84001 (Mittlefehldt 1994; Harvey and McSween 1996). McKay et al. (1996) found that the core regions of the

carbonate globules with more Mg-rich compositions contain relatively few magnetite particles. The observations of Bradley et al. (1996) also indicate that magnetite development within carbonate globules away from the Fe-rich zones is extremely limited. However, from the observations in this study, in comparison, magnetite development appears to be extremely pronounced in the carbonates when they occur as fragments embedded within glass. Similar carbonate compositions apparently contain little magnetite when they occur within globules.

Some discussion exists in the literature as to the exact nature of the feldspathic glass in ALH 84001, in part, because of its unusual and somewhat variable composition (e.g., Mittlefehldt 1994) compared with typical maskelynite in, for example, the shergottite meteorites. McKay et al. (1997) suggested that this phase may, in fact, represent a gel-like material that formed at low temperature from an aqueous solution of some kind. However, no further studies have supported this conjecture, although the silica veins that sometimes crosscut the feldspathic glass certainly do appear to have formed at low temperatures based on their oxygen isotopic composition (Greenwood et al. 2002). Many problems with a low temperature model for the feldspathic glass exist, not least of which is the fact that even at low temperatures, aqueous solutions would be expected to precipitate crystalline albite, as occurs in diagenetic environments (e.g., Saigal et al. 1988; Ramseyer et al. 1992), rather than an amorphous gel-like phase. Further, such a
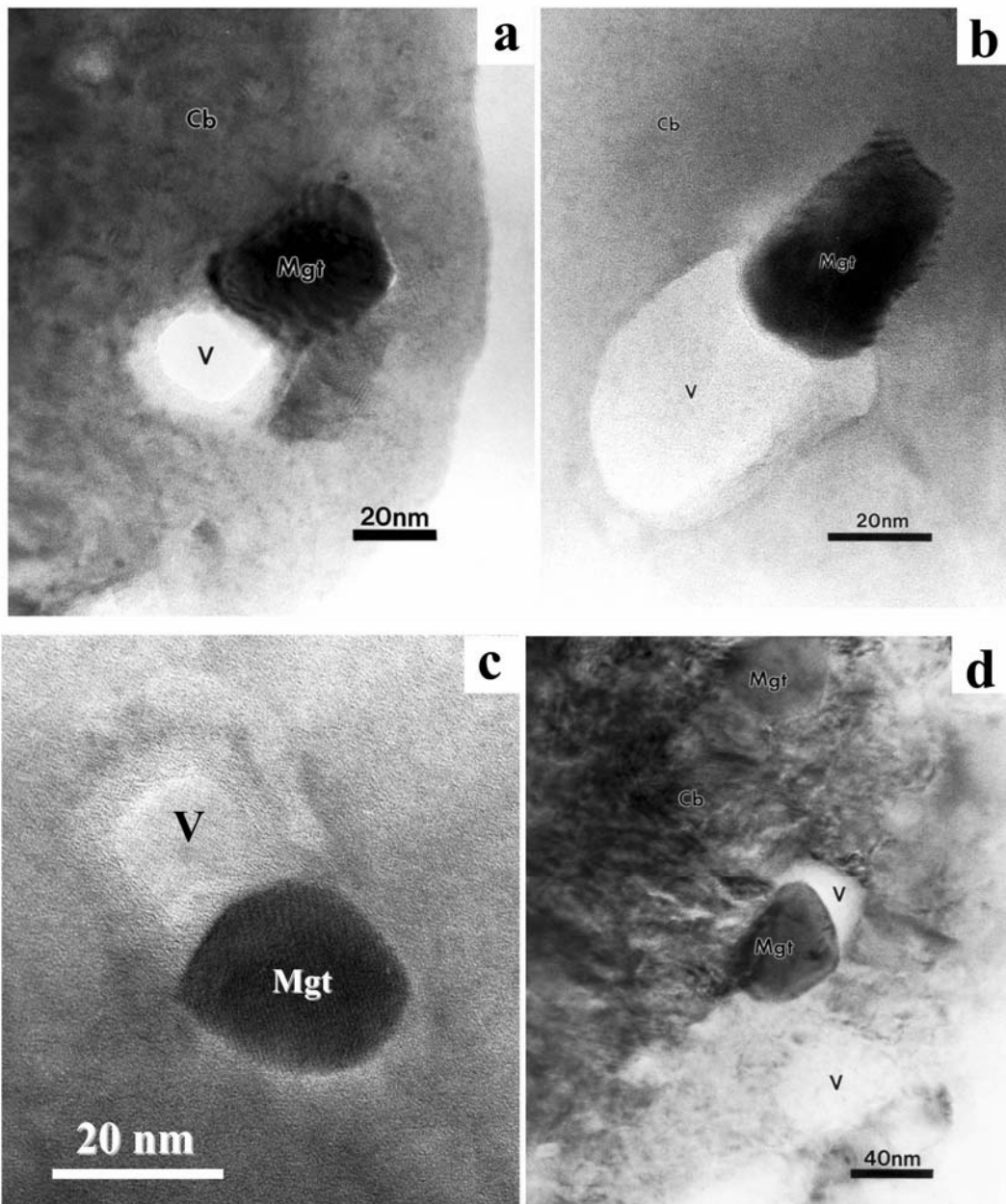
Fig. 10. Bright field transmission electron micrographs showing examples of single magnetite crystals that are commonly associated with voids (V) in carbonate (Cb) fragments in ALH 84001: a) facetted, equant magnetite (Mgt) grain associated with a void; b) elongated magnetite crystal associated with a relatively large void; c) subrounded magnetite crystal that is associated with a small void; d) magnetite associated with an irregularly shaped void.

process would require considerable amounts of water and the resultant gel-like phase would be highly hydrated. The analytical totals for feldspathic glass from ALH 84001 are close to 100%, clearly showing that the water content of this material is extremely low, which is inconsistent with a low temperature origin from an aqueous solution. Additionally, minimal evidence exists of the interaction of water with ALH 84001 that would support formation of the feldspathic glass from aqueous solutions. One could argue that water could

have been lost as a result of mild heating caused, for example, by shock. But, any such process would have resulted in recrystallization of a highly unstable, gel-like phase.

On the other hand, for the feldspathic glass, an extensive body of evidence exists that strongly supports the view that this material has a high temperature origin. First, a body of evidence exists that shows that ALH 84001 experienced shock pressures of ~35–40 GPa, pressures that are expected to form maskelynite from plagioclase (Stöffler 2000), and
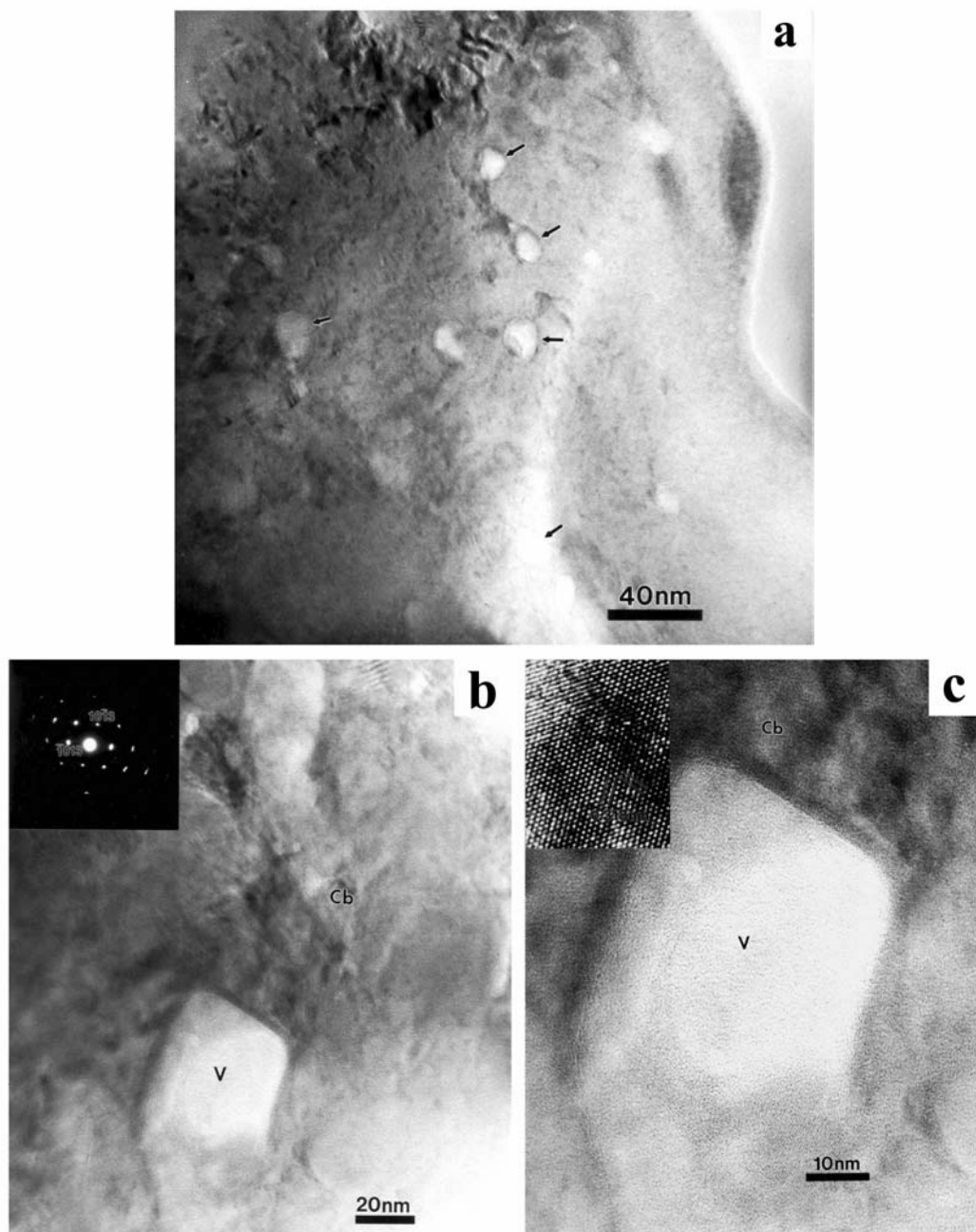
Fig. 11. Transmission electron micrographs of voids in carbonate that are not associated with significant development of magnetite: a) region of carbonate that contains an array of subrounded voids (arrowed); b) image of a region of carbonate that contains a void the shape of which is clearly crystallographically controlled (lower center) and has a rhomb-shaped outline. The inset electron diffraction pattern shows that the walls of the void are the $(10\bar{1}3)$ and $(\bar{1}013)$ planes of the carbonate (i.e. the cleavage planes of rhombohedal carbonates); c) high resolution TEM image of the void shown in (b). The inset (upper left) is an oriented lattice image of the carbonate.

several workers have described textures for the glass that are most consistent with a high temperature origin, i.e., show evidence of injection of glass into adjacent phases (Scott et al. 1997; Greenwood and McSween 2001). A key piece of evidence to resolve the temperature of glass formation would be data on the oxygen isotopic composition of the feldspathic glass because clear differences exist between the oxygen

isotopic composition of high temperature igneous phases and low temperature phases in ALH 84001 (e.g., Valley et al. 1997; Shearer et al. 1999; Greenwood and McKeegan 2002). However, these data are currently not yet available. Nevertheless, irrespective of whether the glass has a high or low temperature origin, a significant amount of evidence exists to show that ALH 84001 experienced significant shock

heating and post igneous crystallization. First, Brearley (1998, 2000) has described phyllosilicates in carbonate inclusions embedded within the feldspathic glass, which show clear evidence of dehydration; and secondly, Scott and Barber (2002) have reported the presence of periclase in carbonate in ALH 84001 that can only have formed by thermal decomposition of carbonate. All these lines of evidence lead to the conclusion that ALH 84001 experienced significant post-shock heating and that the feldspathic glass was formed during these high temperature events.

To understand the microstructural characteristics of the carbonate fragments, one must examine the possible thermal histories of the fragments that occur within the feldspathic glass. The carbonates described above, which occur as fragments within the pockets of feldspathic glass, show clear evidence that they were formed by disruption of larger, pre-existing carbonate masses as a result of shock mobilization (or remobilization) of feldspathic shock melt, as discussed by Shearer and Brearley (1998) and Greenwood and McSween (2001). Although Treiman (1998) has postulated up to 5 shock events for ALH 84001, Greenwood and McSween (2001) have argued that only 2 significant shock events are necessary to explain the textural observations and that the disruption of the carbonates occurred during the second shock event. Evidence of the transport of masses of carbonate within the shock melt during this shock event has been documented (e.g., Shearer and Brearley 1998; Greenwood and McSween 2001). The compositional and zoning characteristics of the carbonates present within pockets of feldspathic glass are essentially identical to those of the carbonate globules and other carbonates within ALH 84001. Indeed, a general agreement exists that all the occurrences of carbonate in ALH 84001 formed under similar conditions and during the same geological event, at ~4.0 Gyr, according to the carbonate dates reported by Borg et al. (1999).

Clearly, invasion of carbonate masses by shock melt and their disruption or fragmentation must have occurred when the shock melt was hot and fluid (Treiman 1998; Shearer and Brearley 1998; Shearer and Adcock 1998). The impact melt would have been injected along planes of weakness in the carbonates (e.g., cleavage planes), and, as noted by Greenwood and McSween (2001), the carbonate has deformed and fragmented in a brittle fashion. During this dynamic process, any carbonate fragments that were incorporated into the shock melt must have been heated to a significant degree. For the case of the carbonate fragments examined in this study, heating is likely to have been especially significant because of their small size and the fact that they are completely entrained within the feldspathic glass. The postshock temperatures reached by plagioclase melts are estimated to be on the order of 900°C (Stöffler et al. 1988). As discussed below, such elevated temperatures, even if the heating event was short-lived, are sufficiently high to have had a significant effect on the carbonates, as indicated by the fact that rare micas that are

sometimes associated with carbonate fragments show evidence of having undergone dehydration due to heating (Brearley 1998; 2000a, b).

I now consider the possible thermal effects of heating on the carbonates in ALH 84001 based on current knowledge of the thermal stabilities of relevant carbonates. Carbonates in ALH 84001 have very unusual compositions. As a consequence, no experimental data exist on the thermal decomposition of carbonate with a composition such as that found in ALH 84001. However, data are available for the thermal stability of several of the important carbonate end members that constitute the carbonate solid solutions in ALH 84001. For the purposes of this discussion, we assume that the thermal decomposition occurs during post-shock heating after pressure release and that pressures during the main decarbonation were probably low, perhaps 500 bars or less. Siderite has been well-established to have a much lower thermal stability than magnesite ($MgCO_3$) or calcite ($CaCO_3$). Specifically, analysis of the thermal decomposition of siderite (Gallagher et al. 1981; Gallagher and Warne 1981) shows that decomposition of siderite in a vacuum can be detected by Mössbauer spectroscopy and by weight loss, even at temperatures as low as 385°C. In a vacuum, wüstite (FeO) is the dominant reaction product, but even at very low PO_2, magnetite is produced (Gallagher et al. 1981). More recent thermogravimetric analyses (Gotor et al. 2000) show that pure siderite begins to decompose at 227°C and, at a heating rate of 0.52 K min^{-1}, has fully decomposed at 287°C. Impurities in siderite expand its thermal stability such that siderite containing 30 mol% magnesite begins to decompose at ~450°C. Phase equilibria studies of the stability of siderite (French 1971) in the pressure range of 500–2000 bars, as a function of temperature and fO_2, show that the thermal stability of siderite increases as a function of increasing pressure, i.e. behavior that is typical for decarbonation reactions. At 500 bars and $\log_{10}fO_2 = -25$, siderite will begin to decompose to magnetite + vapor at 350°C. At $\log_{10}fO_2 = -26$, siderite is stable to a maximum temperature of 450°C (Fig. 12). Golden et al. (2000) have reported data that suggest that siderite breakdown is a function of PCO_2, but at $PCO_2 = 100$ bars, decomposition to magnetite occurs completely at 470°C. All these data show that end member siderite is extremely unstable, even at low temperatures.

In contrast, at 500 bars, magnesite is stable to a temperature of 700°C, based on the experimental data of Harker and Tuttle (1955) and Koziol and Newton (1995). This temperature decreases to about 650°C at 65 bars (Harker and Tuttle 1955). According to the data of Harker and Tuttle (1955), breakdown of calcite occurs at ~985°C (at 7 bars). An additional minor component in solid solution in the ALH 84001 carbonate is rhodocrosite. Under oxygen fugacity conditions for the breakdown of siderite to magnetite + CO_2, rhodocrosite is stable to temperatures of ~550°C at 500 bars (Huebner 1969). These observations show conclusively that
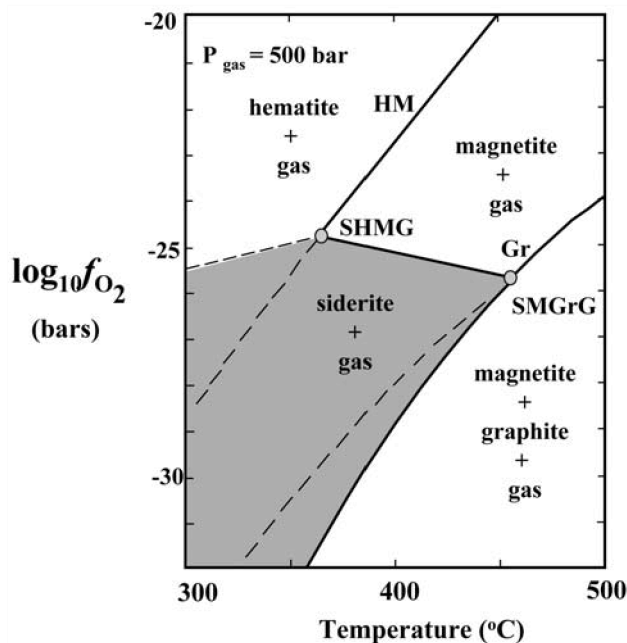
Fig. 12. Phase diagram in the system Fe-C-O showing the stability of siderite (shaded region) in temperature-oxygen fugacity space at P_{gas} = 500 bar (after French 1971).

siderite is much less stable than calcite, magnesite, or rhodocrosite, which are the 3 other significant solid solution components in carbonates in ALH 84001. The observations of Gotor et al. (2000) on siderite that contains 30 mol% magnesite show that the addition of solid solution components will expand the stability field of siderite, but these solid solutions are significantly less stable than end member magnesite and calcite.

Based on these observations, I suggest that during shock heating, the siderite component in solid solution in ALH 84001 carbonates decomposed preferentially and at a significantly lower temperature than either the magnesite, calcite, or rhodocrosite components in solid solution. This type of behavior is extremely common in metamorphic reactions involving the decomposition of solid solutions. For example, during the breakdown of muscovite in pelitic metamorphic rocks, the paragonite component in solid solution in the muscovite decomposes first as temperature increases to produce albite and an aluminosilicate phase. The remaining muscovite moves progressively toward a pure potassium muscovite until the temperature ultimately exceeds the thermal stability of end member muscovite (Evans and Guidotti 1966; Thompson 1974). If such a process does indeed occur in ALH 84001, then formation of the reaction products of siderite breakdown would be expected to be present in carbonates in ALH 84001 that have experienced shock heating. We propose that if shock temperatures were attained for short periods (as would be expected), decomposition of the siderite in the carbonate solid solution could occur without any significant

breakdown of the calcite, magnesite, or rhodocrosite components in the solid solution. The end products of such a process would then be expected to be the products of siderite breakdown within an intact matrix of carbonate that is a solid solution of magnesite and calcite. The preferential breakdown of the siderite component is favored by the fact that its thermal stability is much lower and, hence, the upper stability of siderite will be overstepped by a large temperature interval. Even if the magnesite or calcite upper stability curves were exceeded during the postshock heating, the upper stability of siderite will be overstepped by a much larger temperature interval. Under these conditions, the kinetics of the siderite breakdown reaction will be much faster than for either magnesite or calcite breakdown. Hence, decomposition of either magnesite or calcite components may be kinetically-inhibited and may not occur because of the very short time interval at high temperature available for reaction.

Although no evidence of magnesite decomposition has been observed in any of the fragments examined in this study, Barber and Scott (2002) report nanocrystalline occurrences of periclase associated with Mg-rich carbonate in ALH 84001. In the context of the model proposed here, this observation indicates that, at least locally, temperatures were either higher or the heating episode was longer, allowing decomposition of magnesite to occur. This is consistent with the proposition that thermal excursions caused carbonate decomposition.

The breakdown of siderite to magnetite and CO_2 involves the oxidation of Fe^{2+} to Fe^{3+}, a reaction that is known to occur under fO_2 conditions between the hematite-magnetite and graphite buffers (French 1971). In an oxidizing atmosphere, this reaction can be described as:

$$3FeCO_3 + 0.5O_2 = Fe_3O_4 + 3CO_2$$
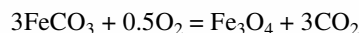
(Gallagher et al. 1981), a reaction that apparently requires the addition of oxygen to the system. However, experimental studies have shown that this is not necessary. Under extremely reducing conditions ($-\log PO_2$ = 29 at 500°C), the breakdown of siderite occurs by the reaction:

$$FeCO_3 = FeO + CO_2$$
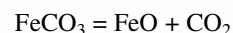
(Gallagher et al. 1981). This first stage in the reaction is also widely recognized in the decomposition of other carbonates such as ankerite and ferroan dolomites (e.g., Iwafuchi et al. 1983; Milodowski et al. 1989; Dubrawski 1991), except that (Mg,Fe)O (magnesiowüstite) is produced during the reaction. In the case of siderite decomposition, FeO (wüstite) is extremely susceptible to oxidation, and in an inert atmosphere (e.g., N_2), the CO_2 released from the breakdown of $FeCO_3$ actually oxidizes the Fe^{2+} to Fe^{3+} due to the dissociation reaction $CO_2 = CO + 0.5O_2$ (Gallagher et al. 1981). And, the overall reaction can be written:

$$3FeCO_3 = Fe_3O_4 + CO + 2CO_2$$

Thus, the decomposition of siderite to magnetite can be accomplished without the addition of oxygen to the system. However, in the case of ALH 84001, water may also have been available, which would act as an oxidizing agent. Small amounts of water could be present either as a hydromagnesite component $(Mg_4[CO_3]_3[OH]_2 \cdot 3H_2O)$ in the carbonate or absorbed along grain boundaries. Alternatively, small amounts of phyllosilicate phases do occur within carbonate fragments (Brearley 1998b, 2000), and these phases have undergone partial dehydration during the shock heating that produced the magnetite. Although not widely distributed, water released from such dehydration reactions could clearly participate in oxidation reactions to form magnetite. Irrespective of the source of water, the decomposition of the siderite component in solid solution in the carbonate, via a decarbonation reaction, is an inescapable consequence of the shock heating of ALH 84001, if shock temperatures exceeded temperatures of ~350°C.

I propose that this hypothesis provides a consistent explanation for a number of the microstructural features of the carbonate fragments, including the ubiquitous association of magnetite with voids that are observed in ALH 84001. This hypothesis can also be extended logically to explain the presence of bands of magnetite in the zoned carbonate globules (McKay et al. 1996), as has been studied experimentally by Golden et al. (2000).

In this model, the abundant voids in the carbonate fragments embedded within feldspathic glass can be explained readily as the consequence of the loss of CO_2 resulting from the decomposition of the siderite component in solid solution in the carbonate. In addition, the very fine-grained character of the magnetite is the result of rapid thermal decomposition caused by the heating associated with the shock melting of the feldspathic glass. In this type of disequilibrium process, where the stability limit of a phase is overstepped by a significant temperature interval, nucleation at many different sites occurs rapidly because the activation energy for nucleation is exceeded for essentially all nucleation sites (Rubie and Thompson 1986; Brearley 1986). Preliminary experimental results of the thermal decomposition of siderite (unpublished data of Brearley) show that, at 900°C, formation of significant amounts of nm-sized magnetite occurs in seconds. In ALH 84001, the heating event was too short-lived to allow any re-equilibration of the complex compositional zoning observed in the carbonate fragments because cation diffusion in carbonates is too sluggish (Fissler and Cygan 1998). The short-lived heating event would also prevent significant growth (coarsening) of the new magnetite crystals.

The highly strained characteristics of the carbonate may also be explained by thermal decomposition of the carbonate. Using the molar volumes for magnetite and siderite, the breakdown of pure siderite to form magnetite by the reaction $3FeCO_3 = Fe_3O_4 + CO + 2CO_2$ results in a volume decrease of the solid phases of almost 50%, a very significant reduction.

Assuming a typical carbonate composition containing 30 mol% siderite in solid solution, of which 20% undergoes decomposition, the volume change would be ~7 vol%. Clearly, not all of this volume change needs to be accommodated if CO_2 is not lost from the grains, but some of the volume reduction will very likely be accommodated by a distortion of the structure in a rather heterogeneous way, depending on where magnetite crystals form. The absence of dislocations indicates that this contraction of the structure is responsible for the highly strained character of the carbonate, rather than shock-induced deformation.

By extension, the thermal decomposition model can also be extended to explain the occurrences of magnetite within the zoned carbonate globules in ALH 84001. In this case, the concentration of magnetite in Fe-rich carbonate bands within zoned carbonate globules, described by McKay et al. (1996) is produced because this Fe-rich carbonate composition is the least thermally stable and will produce the most magnetite on decomposition (e.g., Golden et al. 2000). However, the low abundance of magnetite and voids within other carbonate compositions in the carbonate globules probably result from a thermal gradient across globules such that less Fe-rich carbonate compositions were not heated to sufficiently high temperatures to induce significant decarbonation. In comparison, small carbonate fragments with similar Fe contents, which are surrounded by feldspathic impact melt, were heated to higher temperatures and probably for longer times, because they are completely surrounded by shock melt. As a consequence, the degree of thermal decomposition to magnetite is higher in these grains than in comparable carbonate compositions within larger carbonate globules.

An additional characteristic of carbonate globules in ALH 84001 lends further support to the idea that the magnetites in ALH 84001 could have formed by thermal decomposition. A Fe-rich zone is present on the periphery of most carbonate globules in ALH 84001. As shown in Fig. 13, along the interface between the carbonate globule and the glass, where the Fe-rich zone is present, a well-defined crack or fracture is apparent. However, this fracture is only present where the Fe-rich zone is adjacent to the feldspathic glass. Where glass is in contact with less Fe-rich compositions, no such fracture exists. I suggest that these fractures or cracks are a consequence of the thermal decomposition of a very Fe-rich carbonate zone on the outer region of the carbonate. When the siderite-rich band was heated by the shock melt, it underwent extensive thermal decomposition to magnetite. As discussed above, this would result in a significant volume decrease and would leave a porous aggregate of magnetites with a much lower coherence than the precursor carbonate. This has been demonstrated experimentally by Golden et al. (2000). During sample preparation, this porous zone would be much more susceptible to plucking as a result of polishing, resulting in an apparent fracture along the interface. The presence of the fracture, clearly, is not simply a property of the carbonate
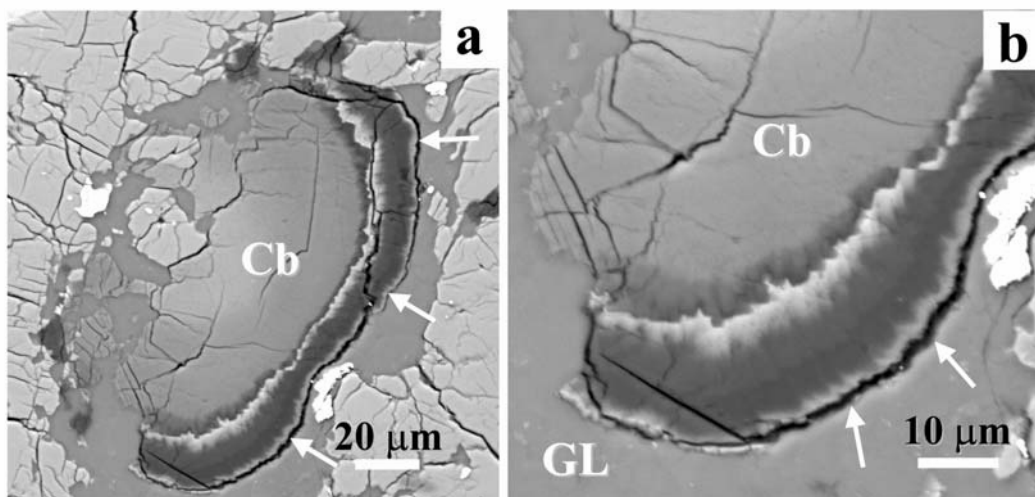
Fig. 13. BSE images of an example of a carbonate globule in ALH 84001 showing the presence of cracks at the interface between the carbonate and the feldspathic glass: a) image of a complete carbonate globule showing the presence of a distinct fracture (arrowed) along the interface between the Fe-rich carbonate and the glass. Note that the fracture is not present on the opposite side of the carbonate where more Mg-rich carbonate is in direct contact with the glass; b) closeup of a region of the interface between the carbonate globule and the glass from the lower part of the image shown in (a). Although present locally, no fracture typically exists at the contact between carbonate and glass on the left side of the image, where the Fe-rich carbonate zone is absent.

interface alone because it is only present where the Fe-rich carbonate zone occurs.

Problems for the Decomposition Model

Thomas-Keprta et al. (2000) have dismissed the possibility that magnetites in ALH 84001 could have formed by thermal decomposition arguing that the elongated prismatic magnetites in ALH 84001 are chemically pure, like magnetites produced by the bacterial strain MV-1. This argument raises 3 important issues that have to be considered when evaluating the thermal decomposition. The first issue is whether or not magnetites in ALH 84001 and MV-1 are really chemically pure. The second issue concerns whether essentially pure magnetite can be produced during the decarbonation of a complex carbonate solid solution that is rich in Mg. The third issue is whether such a complex carbonate solid solution can decompose in steps that are related to the stability of the solid solution components. These issues are considered individually below.

Chemical Purity of ALH 84001 Magnetites

Thomas-Keprta et al. (2000) presented energy dispersive X-ray data that they claimed showed that the elongated prismatic magnetites of putative biogenic origin in ALH 84001 are chemically pure like biogenic magnetite from strain MV-1, while irregular-shaped magnetites in the same meteorite contain significant concentrations of trace elements. Based on an analysis of a standard glass, Thomas-Keprta et al. (2000) estimate that their detection limits of minor elements such as Cr and Fe are of the order of 150 ppm. Using the expression for the minimum mass fraction

detectable by thin film EDS analysis (Williams and Carter 1996) and the estimated integrated peak and background intensities from the spectra of Thomas-Keprta et al. (2000) provides good agreement with this value. However, the experimental conditions for other spectra reported by Thomas-Keprta et al. (2000) are somewhat different from those for the standard spectra. For example, the background intensities for spectra of prismatic elongate magnetites are an order of magnitude lower than those for the standard. (Note that the scale on this figure in Thomas-Keprta et al. [2000] should be Counts $\times$ 10, not Counts $\times$ 10^2.) Background intensities of the standard are about 300 counts per channel versus 25–50 counts per channel. The minimum detection limits will, as a consequence be poorer for these analyses than for those of the standard. A simple calculation assuming a concentration of 1000 ppm Mg in the magnetite and a background intensity of 25 counts per channel, integrated over the peak width (~20 channels), would require total integrated peak counts of ~900 for a detection limit of 500 ppm. Due to the low count rates in the spectrum presented by Thomas-Keprta et al. (2001) and the highly irregular background, determining the position of the background or establishing whether small peaks are present is not possible. A clear suggestion exists that Mg and Al K_α peaks at 1.253 and 1.485 KeV may be present in the spectrum presented by Thomas-Keprta et al. (2000), but the integrated total counts for the peak are ~700, which is below the minimum number of peak counts for detectability. More extended counting times at higher beam currents are necessary to fully determine whether or not these elements are present (Williams and Carter 1996). In conclusion, these data cannot be used to argue unequivocally for or against the presence of minor or

trace concentrations of Mg, Al, etc. in the elongated prismatic magnetites from ALH 84001. Much improved counting statistics are required before any conclusion can be reached about the chemical purity of these grains.

Formation of Magnetite-Rich Spinel During the Decomposition of Mg-Fe-Ca Carbonate Solid Solutions

I now consider the question of the incorporation of Mg into Fe-spinel produced during the decomposition of Mg-bearing carbonates. Under equilibrium conditions, the breakdown products of Fe-bearing, Mg carbonates are largely a function of fO_2: at low fO_2, magnesiowüstite ([MgFe]O) is the stable decomposition product, while at higher fO_2, magnesioferrite ($MgFe^{2+}_2O_4$), sometimes coexisting with hematite, is formed (Chai and Navrotsky 1996; Kang et al. 2000). In these experiments, pure magnetite only occurs as the breakdown product of pure siderite. However, more recent equilibrium studies indicate that this may not always be the case. Koziol (2001) has determined the equilibrium breakdown reaction:

carbonate + hematite = magnetite + CO_2

for pure siderite and siderite$_{60}$magnesite$_{40}$. In the experiments carried out using the siderite-magnesite solid solution, the breakdown product is pure magnetite, based on EDS analysis, not magnesioferrite, contrary to the results of previous studies.

Nevertheless, numerous studies of the kinetics of decomposition of Fe-bearing Mg carbonates indicate that magnesiowüstite forms during the decomposition reaction as an initial step and may be oxidized to magnesioferrite as the reaction proceeds (e.g., Iwafuchi et al. 1983; Milodowski et al. 1989a, b; Dubrawski 1991). These observations would appear to be problematic for the proposed scenario for ALH 84001 documented above, in that they suggest that forming a pure magnetite from the decomposition of an Fe-bearing, Mg-carbonate would not be possible. However, this is a simplistic interpretation that is not necessarily supported by the available data. First, in the thermal regime relevant to the decomposition of carbonate in ALH 84001, equilibrium phase diagrams have only limited relevance because of the high degree of disequilibrium caused by rapid heating and cooling as a result of the shock event. In this situation, the principle of Ostwald's step rule are followed and the kinetics of the reaction, rather than thermodynamics, control the phases and their compositions that form during the reaction (Putnis 1992). Following this principle, one cannot assume, a priori, that the spinel phase, i.e., magnetite in this case, produced during the decomposition of a complex carbonate solid solution will contain Mg, as the equilibrium phase diagram predicts.

At least one documented example exists in the literature that demonstrates the importance of Ostwald's step rule behavior in controlling the composition of spinels produced during decomposition reactions. Brearley (1997) carried out an experimental study of the breakdown of aluminous Mg-Fe biotite under disequilibrium conditions at 800ºC. The stable equilibrium breakdown products of this reaction should be Mg-bearing hercynitic spinel, K-feldspar, and H_2O. However, this experimental study showed that the breakdown of biotite to produce this phase assemblage takes place progressively in a number of different stages. During the initial stages of the reaction (after 48 hours), the spinel phase formed is a submicron hercynitic spinel with a very low Mg but high magnetite content. As a function of time, the Mg-content of the spinel progressively increases until, after several days, a hercynitic spinel with the equilibrium Mg/(Mg + Fe) ratio is finally produced. Other experiments, carried out for shorter periods (unpublished data of Brearley), show that the very earliest stages of the breakdown reaction involve the formation of myriad nm-sized crystals of pure magnetite. These experiments demonstrate that, under disequilibrium conditions, the earliest phase that forms is the one which is kinetically the easiest to nucleate, in this case, a simple binary oxide rather than a more complex solid solution. However, with time, this metastable composition evolves towards that of the stable equilibrium phase.

These experiments demonstrate that the use of equilibrium phase diagrams to predict the compositions of product phases during disequilibrium reactions is flawed. In addition, they also demonstrate the principle that Fe-rich phases with little or no Mg can be formed as metastable phases during the very earliest stages of decomposition reactions under disequilibrium conditions.

As discussed above, a number of studies have been conducted on the thermal decomposition of Fe-bearing Ca-Mg carbonates, such as ferroan dolomite or ankerite. These studies have been carried out using differential thermal analysis (DGA), thermogravimetric analysis (TGA), and other related techniques (e.g., Iwafuchi et al. 1983; Milodowski et al. 1989a; Dubrawski 1991; Gotor et al. 2000). In these studies, crushed samples of carbonates are heated progressively at rates of 10–15ºC min^{-1} from room temperature to above the final decomposition temperature of the carbonate (typically 1000ºC), and the weight loss as a function of time is measured as an indicator of the degree of decarbonation of the sample. Although considerable discussion exists in the literature as to mechanisms of the decomposition reactions and the product phases (see, for example, Milodowski et al. 1989), most authors argue that magnesiowüstite or periclase is formed as an intermediate phase (as discussed above). This step is followed by a Fe-rich spinel phase that is postulated to contain a significant component of Mg in solid solution as magnesioferrite ($Mg_2Fe^{3+}O_4$) (e.g., Iwafuchi et al. 1983). However, as pointed out by a number of workers (e.g., Iwafuchi et al. 1983; Milodowski et al. 1989), a considerable degree of uncertainty exists as to the nature of these phases and their compositions, because periclase, magnesiowüstite, magnesioferrite,

magnetite, and their solid solutions have virtually identical X-ray diffraction patterns. Indeed, these uncertainties in the exact nature of the decomposition products are partially responsible for the differences in mechanisms that have been proposed for the breakdown of Fe-bearing carbonates in the literature. Hence, although a magnetite-magnesioferrite solid solution may be expected to form during the decomposition reaction, this has not, in fact, been demonstrated in most TGA/DGA studies, because direct compositional data from, for example, analytical electron microscopy has not been performed on the experimental run products.

Mössbauer spectroscopic studies (e.g., Milodowski et al. 1989) provide some evidence to support the argument that magnetite is not the breakdown product during the first stage of ankerite decomposition. Milodowski et al. (1989) showed that the Mössbauer spectrum of the decomposition residue of ankerite heated to 740–750ºC is certainly not magnetite but could be maghemite or magnesioferrite. However, based on X-ray diffraction data, they concluded that this phase was most consistent with the latter. Clearly compositional data obtained by analytical electron microscopy would be extremely useful in helping to evaluate the degree to which Mg (as magnesioferrite $Mg_2Fe^{3+}O_4$) enters the magnetite decomposition product of Fe-bearing Mg-Ca carbonates.

Although the Mössbauer data support the view that magnesioferrite is the final decomposition product, they do not provide any insights into the very earliest stages in the thermal decomposition of ankerite or other Fe-bearing carbonates. All the XRD and Mössbauer studies are invariably carried out on the products of relatively high temperature runs where decomposition of the Fe-bearing component of the carbonate is extremely advanced, i.e., on samples that have been heated to 700ºC and above. At the typical heating rates of such studies, the samples will, therefore, have spent several minutes above 500ºC, a thermal history which is dramatically different from that envisaged for shock heating of carbonates in ALH 84001. For example, Milodowski et al. (1989b) performed their Mössbauer experiments on samples that were heated to 740–750ºC, almost 80ºC above the temperature at which the TGA data show that decarbonation had commenced. In the case of the carbonate in ALH 84001, the carbonate clearly contains a significant amount of Fe, indicating that if the decomposition model is correct, the breakdown reaction is only at its very earliest stages.

The importance of kinetics on the decomposition products of ferran dolomite and ankerite has also been emphasized by the experimental data of Milodowski et al. (1989a). These authors note that the mechanism of decomposition of the carbonate is highly dependent on the heating rate used for the experiment. At high rates of heating, an intermediate spinel phase is produced that has a significant Fe^{2+} content, while at slow heating rates, magnesioferrite with no Fe^{2+} in solid solution is produced. This observation is interpreted as being the result of high P_{CO} during rapid

heating, which favors the metastable formation of Fe^{2+}-rich spinel phases such as magnetite. Given that the heating rates used in the TGA experiments of Milodowski et al. (1989a) are significantly slower than would have been the case for the shock heating of ALH 84001, this type of effect is likely to be even more dramatic during rapid heating.

More recent data on the isothermal decomposition of siderite-magnesite solid solutions (Golden et al. Forthcoming) also indicate that the Fe-spinel that forms need not contain significant concentrations of Mg. Golden et al. (Forthcoming) examined the composition of magnetites produced from the thermal decomposition of carbonate synthesized from hydrothermal solutions containing 75 mol% Mg. In these experiments, a few magnetites contained no detectable Mg <~0.3 wt%), while many contained detectable Mg. These observations indicate that even when decomposition of an Mg-bearing carbonate is significant, the spinel decomposition products do not necessarily take up much Mg in solid solution.

In summary, under equilibrium conditions and during slow heating, the decomposition of Fe-bearing, Mg-carbonate should result in the formation of an Mg-bearing, Fe-spinel of some kind. However, in the case of the carbonates in ALH 84001, kinetics are the dominant controlling factor because of the extreme disequilibrium conditions. Further, the thermal decomposition experiments carried out on Fe-bearing, Mg-carbonates do not provide definitive evidence that Mg-bearing spinel phases must be formed, because of the problems of distinguishing between a number of different spinel phases with virtually identical X-ray diffraction patterns. Finally, none of these experiments replicate the postulated thermal history of carbonates in ALH 84001 because phase identification was performed on samples that spent relatively extended periods of time at elevated temperatures and have undergone extensive decomposition. These experiments, therefore, provide no information on the very earliest stages of incipient decomposition of carbonates and cannot be used to definitively argue for or against the shock decomposition model. At present, no experimental data exist in the literature that preclude the formation of pure magnetite during the very earliest stages of thermal decomposition of a complex Mg-Fe-Ca carbonate solid solution.

Progressive Decomposition of Carbonate Solid Solutions

The third issue concerns the question of whether a complex carbonate solid solution can undergo progressive decomposition such that one component in solid solution breaks down without the entire phase decomposing. A substantial body of experimental data exists that indicates that this is a process that certainly occurs during the decomposition of carbonate solid solutions, although further experimental work to clarify detailed mechanisms are still required. Graf and Goldsmith (1955) studied the PCO_2-T phase equilibria of dolomite and Mg-calcite and found that, at equilibrium (PCO_2 = 1 atm), dolomite decomposed into

periclase and Mg-rich calcite with 6 mol% $MgCO_3$ in solid solution. The amount of $MgCO_3$ in solid solution was found to increase with increasing PCO_2. Milodowski et al. (1989a) also found that the decomposition of ferran dolomite and ankerite results in the formation of an Mg-bearing calcite in addition to other decomposition products, although, significant differences exists in the interpretation of the data.

The bulk of the data to support progressive decomposition of a carbonate solid solution comes from thermogravimetric-differential thermogravimetric (TG-DTG) studies of the behavior of Fe-bearing carbonates. Numerous examples of such studies exist in the literature (e.g., Beck 1950; Kulp et al. 1951; Dasgupta 1967; Iwafuchi et al. 1983, Milodowski et al. 1989), but the behavior of ferromanganoan dolomite (Iwafuchi et al. 1983) and carbonates in the dolomite-ferroan, dolomite-ankerite series (Milodowski et al. 1989a) exemplify the decomposition behavior of complex carbonate solid solutions. Both studies show that the decomposition of dolomite and ankerite is complex and involves distinct stages of CO evolution, indicating that decomposition is taking place in different stages. For the case of the decomposition of Fe-bearing carbonates such as Fe dolomite, Fe-Mn dolomite, and ankerite in flowing CO_2, both studies show 3 distinct CO_2 evolution peaks as temperature is increased. Based on X-ray diffraction data, the first peak is interpreted in both studies as representing the breakdown of both $FeCO_3$ and $MgCO_3$ components, leaving the $CaCO_3$ component intact. Iwafuchi et al. (1983) argue that the final reaction products in their study are $CaCO_3$, $(Fe, Mn)_3O_4$ and MgO, whereas Milodowski et al. (1989a) suggest that calcite and magnesioferrite are the end products of the reaction. In both cases, a significant solid solution of Mg appears to exist in calcite. Both of these studies demonstrate that preferential decomposition of one or two carbonate components (i.e., $FeCO_3$, $MgCO_3$) can occur, leaving the third ($CaCO_3$) intact. However, neither study discusses the possibility that the $FeCO_3$ component might decompose before $MgCO_3$. Nevertheless, as discussed earlier, evidence exists in the study of Milodowski et al. (1989a) that such a process can occur. This is indicated by thermomagnetometry of the thermal decomposition products of ankerite, which show that the Fe^{2+} content of the spinel reaction product increases as a function of heating rate. These observations support the hypothesis that at very fast heating rates, kinetics play a very important role and that the formation of a magnetite-rich spinel would be favored over a more complex phase such as magnesioferrite.

Further evidence for the preferential decomposition of the Fe-bearing component in magnesite-siderite solid solutions comes from the experimental studies of Koziol (2001) and Koziol and Brearley (2002). As noted earlier, Koziol (2001) found that during the breakdown of a siderite-magnesite solid solution + hematite, pure magnetite was formed, rather than Mg-bearing spinel. Koziol and Brearley (2002) heated carbonates with compositions along the

siderite-magnesite join at 470ºC for 5 min and studied the resultant phases studied with X-ray diffraction. These studies show that partial decomposition of the carbonate had occurred, producing a Fe-rich spinel phase and a magnesite-siderite solid solution. Detailed analysis of the cell volume of the carbonate shows that there is a unit cell contraction of between 0.27 and 1.09%, with higher degrees of contraction observed at more siderite-rich compositions. These observations demonstrate that the magnesite component of the carbonate is stable under these conditions and that preferential decomposition of the siderite end member in solid solution is occurring, driving the remaining carbonate to more Mg-rich compositions (and lower cell volumes). Presently, no analytical data exist to show that the breakdown products are pure magnetite; however, the results clearly prove that the principle of partial decomposition of one component of the carbonate is occurring at these conditions.

Magnetite Morphology

Extensive discussion exists in the literature over the importance of the morphology of the magnetites in ALH 84001 as an indicator of their biogenicity (e.g., Thomas-Keprta et al. 2000, 2001). This discussion has focused on a subset of the magnetites that are elongated prisms with hexagonal cross-sections, which constitute ~27% of the magnetites present (Thomas-Keprta et al. 2000, 2001). According to Thomas-Keprta et al. (2000), "the elongated prismatic ALH 84001 magnetites show chemical and physical characteristics that have no analog in either the abiotic terrestrial or extraterrestrial database." This statement has been progressively weakened as a result of recent studies on the thermal decomposition of Fe-bearing carbonate. Experimental work on the thermal decomposition of Fe-Mg carbonates (Golden et al. 2000; Koziol and Brearley 2002; Golden et al. Forthcoming) show conclusively that the breakdown products are nanophase magnetites with size ranges that match those of magnetites in ALH 84001. Despite the assertions of Thomas-Keprta et al. (2002) to the contrary, detailed comparisons of the morphologies of magnetites in ALH 84001 with those produced by magnetotactic bacteria strain MV-1 and thermal decomposition show that there are remarkable similarities between them (Golden et al. Forthcoming). In detail, the ALH 84001 magnetites appear to match most closely those produced by thermal decomposition, although, the differences are quite subtle (Golden et al. Forthcoming). As a consequence, the arguments for a biological origin for a subset of magnetites in ALH 84001 have been significantly weakened, if not fully disproven.

One major weakness in the arguments presented by Thomas-Keprta et al. (2001) is the fact that the majority of the population of the magnetites in ALH 84001 have morphologies that are not consistent with a biological origin. The irregular, cuboid, and teardrop morphologies that make

up the bulk of magnetites in ALH 84001 clearly have an inorganic origin and this morphological diversity is readily produced during the experimental isothermal decomposition of Fe-bearing carbonate (Golden et al. 2001). As discussed above, unequivocal evidence exists that ALH 84001 has experienced extensive shock that would have resulted in significant shock heating, i.e., evidence for shock pressures in excess of >35 GPa (Stöffler 2000; Barber and Scott 2001), the formation of periclase (Scott and Barber 2002), and the dehydration of phyllosilicates in the feldspathic glass (Brearley 1998, 2000). The carbonate fragments embedded in feldspathic glass must have been heated during the shock event(s), and the formation of magnetite under these conditions is essentially unavoidable. Application of the principle of Occam's Razor, therefore, leads us logically towards the simplest explanation of the observations: all the magnetites were produced by the same mechanism, i.e., thermal decomposition of Fe-bearing carbonates, a conclusion also reached by Barber and Scott (2002).

Given that magnetites with different morphologies are produced in isothermal experiments, one would expect that a wide range of magnetite morphologies would be observed in carbonates in ALH 84001 as a consequence of the extreme thermal regime under which the magnetites grew. A post shock thermal pulse would produce a rapid rise in temperature above the thermal stability limit of siderite, followed by a slower, but still rapid, cooling period. Consequently, the growth conditions for the magnetites would be changing drastically throughout the period that magnetite growth was occurring. At high temperatures, growth would be extremely rapid and some decomposition of the Fe-bearing component would take place, but only for a very short period of time. Under these conditions, growth of magnetite grains might occur essentially unrestricted in rapidly developing voids, produced by CO_2 loss. However, as the temperature dropped, the rate of carbonate decomposition would decrease, and the crystal structure of the carbonate would exert a much stronger constraint on the morphology of the magnetite that formed. The process of magnetite formation in this model is, therefore, extremely complex and involves growth of magnetite under extreme and, indeed, variable degrees of disequilibrium, as a result of rapidly changing conditions. In this model, the platelet and whisker magnetites formed by condensation (Bradley et al. 1996) represent the result of extreme localized shock heating that caused some volatilization at peak post shock temperatures.

CONCLUSIONS

Feldspathic glass pockets in ALH 84001 frequently contain regions of carbonate fragments that have formed as a result of disruption of larger carbonate masses caused by the mobilization and injection of feldspathic carbonate melt. TEM studies of these carbonate fragments show that the carbonates have a complex microstructure. In addition to

being highly strained, the carbonate grains are characterized by the presence of myriad nm-sized magnetite crystals that are frequently associated with voids. All the magnetite morphologies that have been described previously are present within the carbonate fragments. These features are interpreted as being the result of thermal decomposition of Fe-bearing carbonate as a result of shock heating. Post-shock temperatures for feldspathic glasses are likely to be of the order of 900ºC, such that the carbonate fragments must have experienced heating during their dispersion within the melt phase. An inescapable consequence of this heating is that the carbonates would have undergone partial thermal decomposition. Based on a consideration of the relative thermal stabilities of siderite, magnesite, and calcite, the principle end member carbonates in ALH 84001 carbonates, the magnetite and voids in the carbonate fragments are proposed to have formed by preferential decomposition of the siderite component in solid solution in the carbonate under extreme disequilibrium conditions, which would favor formation of magnetite over magnesioferrite.

Applying the principle of Occam's Razor, a reasonable conclusion is that all the magnetites in ALH 84001 were formed by such a mechanism, rather than different mechanisms for spatially-associated magnetites, as is required by existing models (i.e., inorganic mechanisms for ~73% of the magnetites and biogenic for the remaining 27%) proposed by Thomas-Keprta et al. (2000). The experimental results reported by Golden et al. (2001, Forthcoming) provide strong evidence to support this hypothesis, but more extensive studies on the mechanisms and textures of siderite and siderite-bearing solid solution breakdown reactions are necessary to fully validate or disprove this hypothesis.

Editorial Handling—Dr. Joseph Goldstein

REFERENCES

Barber D. J. and Scott E. R. D. 2001. Transmission electron microscopy of carbonates and associated minerals in ALH 84001: Impact-induced deformation and carbonate decomposition. *Meteoritics & Planetary Sciences* 36:A13.

Barber D. J. and Scott E. R. D. 2002. Origin of supposedly biogenic magnetite in the martian meteorite Allan Hills 84001. *Proceedings of the National Academy of Sciences* 99:6556–6561.

Beck C. W. 1950. Differential thermal analysis curves of carbonate minerals. *American Mineralogist* 35:985–1013

Blake D., Treiman A., Cady S., Nelson C., and Krishnan K. 1998. Characterization of magnetite within carbonate in ALH 84001 (abstract #1347). 29th Lunar and Planetary Science Conference. CD-ROM.

Borg L. E., Connelly J. N., Nyquist L. E., Shih C. Y., Wisemann H., and Reese Y. 1999. The age of the carbonates in martian meteorite ALH 84001. *Science* 286:90–94.

Bradley J. P., Harvey R. P., and McSween H. Y., Jr. 1996. Magnetite whiskers and platelets in the ALH 84001 martian meteorite: Evidence of vapor phase growth. *Geochimica et Cosmochimica Acta* 60:5149–5155.

Bradley J. P., McSween H. Y., Jr., and Harvey R. P. 1998. Epitaxial growth of nanophase magnetite in martian meteorite Allan Hills 84001: Implications for biogenic mineralization. *Meteoritics & Planetary Science* 33:765–773.

Brearley A. J. 1986. An electron optical study of muscovite breakdown in pelitic xenoliths during pyrometamorphism. *Mineralogical Magazine* 50:385–397.

Brearley A. J. 1998a. Magnetite in ALH 84001: Product of the decomposition of ferroan carbonate (abstract #1451). 29th Lunar and Planetary Science Conference. CD-ROM.

Brearley A. J. 1998b. Rare K-bearing mica in Allan Hills 84001: Additional constraints on carbonate formation. *LPI Contribution No. 956.* p. 6.

Brearley A. J. 2000. Phyllosilicates in ALH 84001: Constraints on a martian origin from TEM observations. *Geological Society of America Abstracts with Programs* 32:A239.

Dasgupta D. R. 1967. Thermal decomposition of dolomite and ankerite. *Mineralogical Magazine* 36:138–141

Dubrawski J. V. 1991. Thermal decomposition of some siderite-magnetite minerals using DSC. *Journal of Thermal Analysis* 37:1213–1221.

Evans B. W. and Guidotti C. V. 1966. The sillimanite-potash feldspar isograd in western Maine, USA. *Contributions to Mineralogy and Petrology* 12:25–62.

Fissler D. K. and Cygan R. T. 1998. Cation diffusion in calcite: Determing closure temperatures and the thermal history for the Allan Hills 84001 meteorite. *Meteoritics & Planetary Science* 33:785–789.

French B. M. 1971. The stability of siderite ($FeCO_3$) in the system Fe-C-O. *American Journal of Science* 271:37–78.

Gallagher P. K. and Warne S. St. J. 1981. Thermomagnetometry and thermal decomposition of siderite. *Thermochimica Acta* 43:254–267.

Gallagher P. K., West K. W., and Warne S. St. J. 1981. Use of the Mössbauer effect to study the thermal decomposition of siderite. *Thermochimica Acta* 50:41–47.

Gleason J. D., Kring D. A., Hill D. H., and Boynton W. V. 1997. Petrography and bulk chemistry of martian orthopyroxenite ALH 84001: Implications for the origin of secondary carbonates. *Geochimica et Cosmochimica Acta* 61:3503–3512.

Golden D. C., Ming D. W., Schwandt C. S., Morris R. V., Yang S. V., and Lofgren G. E. 2000. An experimental study on kinetically-driven precipitation of Ca-Mg-Fe carbonates from solution: Implications for the low temperature formation of carbonates in martian meteorite ALH 84001. *Meteoritics & Planetary Science* 35:457–465.

Golden D. C., Ming D. W., Schwandt C. S., Lauer H. V., Socki R. A., Morris R. V., Lofgren G. E., and McKay G. A. 2001. A simple inorganic process for formation of carbonates, magnetite, and sulfides in martian meteorite ALH 84001. *American Mineralogist* 86:370–375.

Golden D. C., Ming D. W., Morris R. V., Brearley A. J., Lauer H. V., Jr., Bazylinsky D. A., Treiman A., Zolensky M. E., Schwandt C. S., Lofgren G. E., and McKay G. A. Forthcoming. Morphology of [111]-elongated magnetite crystals in martian meteorite ALH 84001, magnetotactic bacterial strain MV-1, and thermal decomposition of hydrothermally precipitated Fe-rich carbonate: Evidence for inorganic-only formation of magnetite in the martian meteorite. *American Mineralogist.*

Goldstein J. I, Newbery D. E., Echlin P., Joy D. C., Romig A., Jr., Lyman C. E., Fiori C., and Lifshin E. 1992. *Scanning electron microscopy and X-ray microanalysis: A text for biologists, materials scientists, and geologists.* New York: Plenum Press. 820 p.

Gotor F. J., Macias M., Ortega A., and Criado J. M. 2000. Comparative study of the kinetics of the thermal decomposition of synthetic and natural siderite samples. *Physics and Chemistry of Minerals* 27:495–503.

Greenwood J. P. and McKeegan K. D. 2002. Oxygen isotopic composition of silica in ALH 84001. *Meteoritics & Planetary Science* 37:A58.

Greenwood J. P. and McSween H. Y., Jr. 2001. Petrogenesis of Allan Hills 84001: Constraints from impact-melted feldspathic and silica glasses. *Meteoritics & Planetary Science* 36:43–61.

Harker R. I. and Tuttle O. F. 1955. Studies in the system CaO-MgO-CO_2: Part 1. The thermal dissociation of calcite, dolomite, and magnesite. *American Journal of Science* 253:209–224.

Harvey R. P. and McSween H. Y., Jr. 1996. A possible high temperature origin for the carbonates in the martian meteorite ALH 84001. *Nature* 382:49–51.

Huebner J. S. 1969. Stability relations of rhodocrosite in the system manganese-carbon-oxygen. *American Mineralogist* 54:457–481.

Williams D. B and Carter C. B. 1996. *Transmission electron microscopy: A textbook for material science.* New York: Plenum Press. 729 p.

Koziol A. M. 2001. A siderite-magnesite decomposition study (abstract). *Geological Society of America Abstracts with Programs* 33:311.

Koziol A. M. and Brearley A. J. 2002. A non-biological origin for the nanophase magnetite grains in ALH 84001: Experimental results (abstract #1672). 33rd Lunar and Planetary Science Conference. CD-ROM.

Koziol A. M. and Newton R. C. 1995. Experimental determination of the reactions magnesite + quartz = enstatite + CO_2 and magnesite = periclase + CO_2, and the enthalpies of formation of enstatite and magnesite. *American Mineralogist* 80:1252–1260.

Kring D. A., Swindle T. D., Gleason J. D., and Krier J. A. 1998. Formation and relative ages of maskelynite and carbonate in the martian meteorite ALH 84001. *Geochimica et Cosmochimica Acta* 62:2155–2166.

Kulp J. L., Kent P., and Kerr P. F. 1951. Thermal study of the Ca-Mg-Fe carbonate minerals. *American Mineralogist* 36:643–670.

McKay D. S., Gibson E. K. J., Thomas-Keprta K. L., Vali H., Romanek C. S., Clemett S. J., Chillier X. D. F., Maechling C. R., and Zare R. N. 1996. Search for past life on Mars: Possible relic biogenic activity of martian meteorite ALH 84001. *Science* 273:924–930.

McKay G. A and Lofgren G. E. 1997. Carbonates in ALH 84001: Evidence of kinetically-controlled growth (abstract). *Meteoritics & Planetary Science* 28:921–922.

McKay G. A., Mikouchi T., and Lofgren G. E. 1997. Carbonate and feldspathic glass in Allan Hills 84001: Additional complications (abstract). *Meteoritics & Planetary Science* 32:A87.

Milodowski A. E., Morgan D. J., and Warne S. St. J. 1989a. Thermal

analysis of studies of the dolomite-ferroan dolomite-ankerite series. II. Decomposition mechanism in flowing CO_2 atmosphere. *Thermochimica Acta* 152:279–297.

Milodowski A. E., Goodman B. A., and Morgan D. J. 1989b. Mössbauer spectroscopic study of the decomposition mechanism of ankerite in CO_2 atmosphere. *Mineralogical Magazine* 53:465–471.

Mittlefehldt D. W. 1994. ALH 84001, a cumulate orthopyroxenite member of the SNC meteorite group. *Meteoritics* 29:214–221.

Putnis A. 1992. Introduction to mineral sciences. Cambridge: Cambridge University Press. 457 p.

Ramsayer K., Bole. J. R., and Lichtner P. C. 1992. Mechanism of plagioclase albitization. *Journal of Sedimentary Petrology* 59:361–374.

Rubie D. C. and Thompson A. B. 1985. Kinetics of metamorphic reactions at elevated temperatures and pressures: An appraisal of available experimental data. In *Metamorphic reactions; Kinetics, textures, and deformation,* Vol. 4., edited by Thompson A. B. and Rubie D. C. New York: Springer Verlag. pp. 27–79.

Saigal G. C., Morad S., Bjorlykke K., Egeberg P. K., and Aargaaard P. 1988. Diagenetic albitization of detrital K-feldspar in Jurassic, Lower Cretaceous, and Tertiary clastic reservoir rocks from offshore Norway, I. Textures and origin. *Journal of Sedimentary Petrology* 58:1003–1013.

Scott E. R. D., Krot A. N., and Yamaguchi A. 1998. Carbonates in fractures of martian meteorite Allan Hills 84001: Petrologic evidence for impact origin. *Meteoritics & Planetary Science* 33:709–719.

Scott E. R. D., Yamaguchi A., and Krot A. N. 1997. Petrological evidence for shock melting of carbonates in the martian meteorite ALH 84001. *Nature* 387:366–379.

Shaffer P. T. B. 1967. Whiskers—Their growth and properties. In *Modern composite materials,* edited by Broutman L. J. and Brock B. H. Reading: Addison-Wesley Publishing Company. pp. 197–216.

Shearer C. K. and Adcock C. T. 1998. The relationship between the carbonate and shock produced glass in ALH 84001 (abstract #1754). 29th Lunar and Planetary Science Conference. CD-ROM.

Shearer C. K. and Brearley A. J. 1998. Evidence for a late-stage thermal overprint in Allan Hills 84001 and implications for biomarkers. Martian meteorites: Where do we stand and where are we going? *LPI Contribution No. 956.* pp. 47–49.

Shearer C. K., Spilde M. N., Wiedenbeck M., and Papike J. J. 1997. The petrogenetic relationships between carbonates and pyrite in martian meteorite ALH 84001. 28th Lunar and Planetary Science Conference. pp. 1293–1294.

Shearer C. K., Leshin L. A., and Adcock C. T. 1999. Olivine in martian meteorite Allan Hills 84001: Evidence for a high-temperature origin and implications for signs of life. *Meteoritics & Planetary Science* 34:331–339.

Stöffler D. 2000. Maskelynite confirmed as a diaplectic glass: Indication for peak shock pressures below 45 GPa in all martian meteorites (abstract #1170). 31st Lunar and Planetary Science Conference. CD-ROM.

Stöffler D., Bischoff A., Buchwald V., and Rubin A. E. 1988. Shock effects in meteorites. In *Meteorites and the early solar system,* edited by Kerridge J. F. and Matthews M. S. Tucson: University of Arizona Press. pp. 165–202.

Thomas-Keprta K. L., Bazylinski D. A., Kirschvink J. L., Clemett S. J., McKay D. S., Wentworth S. J., Vali H., Gibson E. K., and Romanek C. S. 2000. Elongated prismatic magnetite crystals in ALH 84001 carbonate globules: Potential martian magnetofossils. *Geochimica et Cosmochimica Acta* 64:4049–4081.

Thomas-Keprta K. L., Clemett S. J., Bazylinski D. A., Kirschvink J. L., McKay D. S., Wentworth S. J., Vali H., Gibson E. K., McKay M. F., and Romanek C. S. 2001. Truncated hexa-octahedral magnetite crystals in ALH 84001: Presumptive biosignatures. *Proceedings of the National Academy of Sciences* 98:2164–2169.

Thompson A. B. 1974. Calculation of muscovite-paragonite-alkali feldspar phase relations. *Contributions to Mineralogy and Petrology* 44:173–194.

Treiman A. H. 1995. A petrographic history of martian meteorite ALH 84001: Two shocks and an ancient age. *Meteoritics* 30:294–302.

Treiman A. H. 1998. The history of ALH 84001 revised: Multiple shock events. *Meteoritics & Planetary Science* 33:753–764.

Valley J. W., Eiler J. M. Graham C. M., Gibson E. K., Romanek C. S., and Stolper E. M. 1997. Low-temperature carbonate concretions in the martian meteorite ALH 84001: Evidence from stable isotopes and mineralogy. *Science* 275:1633–1638.

Veblen D. R. and Post J. E. 1983. A TEM study of fibrous cuprite (chalcotrichite): Microstructures and growth mechanisms. *American Mineralogist* 68:790–803.